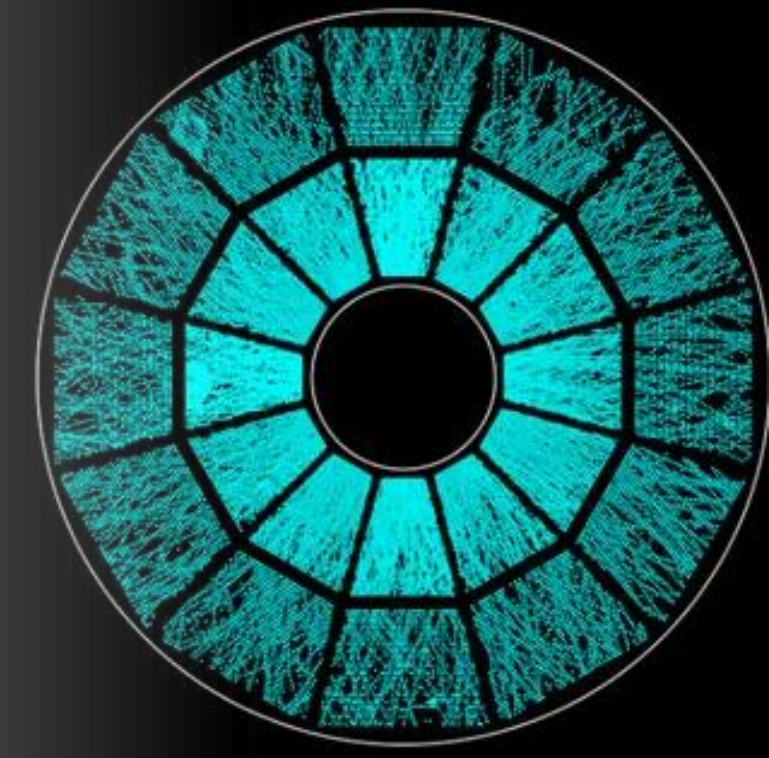
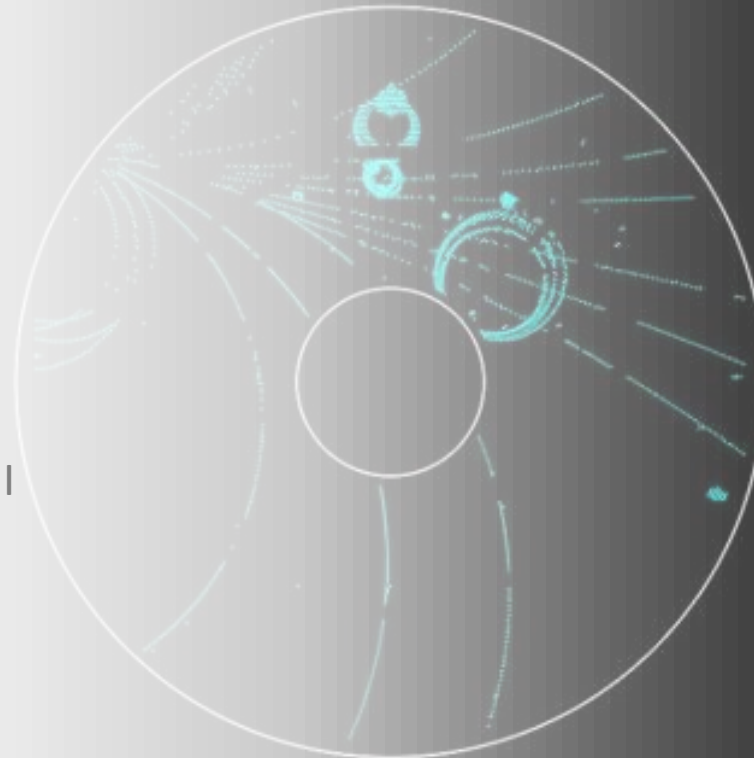




# Measuring Global Observables in the STAR Experiment

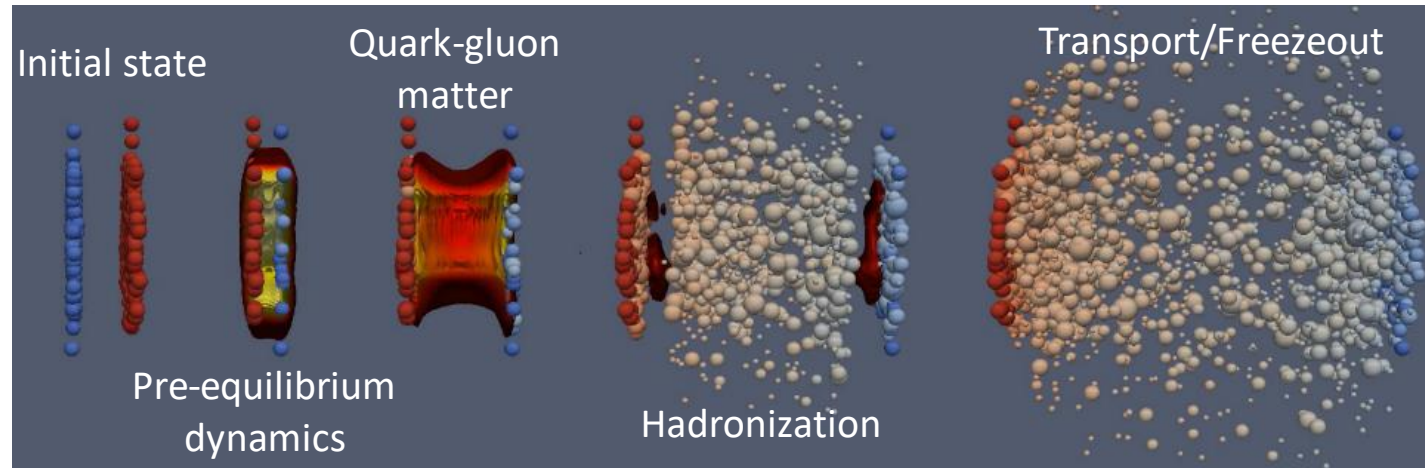
Grigory Nigmatkulov<sup>1,2</sup>

1. National Research Nuclear University MEPhI (Moscow Engineering Physics Institute)
2. Joint Institute for Nuclear Research





# Collision Evolution



- Non-equilibrium evolution at early times
  - initial state at from QCD? Color Glass Condensate? ...
  - thermalization via strong interactions, plasma instabilities, particle production, ...
- Local thermal and chemical equilibrium
  - strong interactions lead to short thermalization times
  - evolution from relativistic fluid dynamics
  - expansion, dilution, cool-down
- Chemical freeze-out
  - for small temperatures one has mesons and baryons
  - inelastic collision rates become small
  - particle species do not change any more
- Thermal freeze-out
  - elastic collision rates become small
  - particles stop interacting
  - particle momenta do not change any more

## System properties can be probed via:

- Transverse momentum particle spectra
- Momentum and angular correlations
- Azimuthal anisotropies
- Global and local polarization of particles
- Jet spectrum and shapes
- Fluctuation of conserved charges
- Etc...

# Some definitions

## Kinematics

- *Pseudorapidity*,  $\eta$ , is used to describe polar angle (z-y plane):  
$$\eta \equiv -\ln\left(\tan\frac{\theta}{2}\right)$$
- $\eta$  is a good approximation of to the *rapidity*,  $y$ :

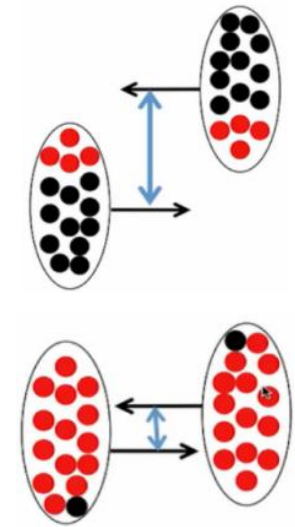
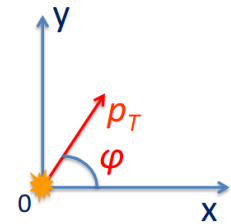
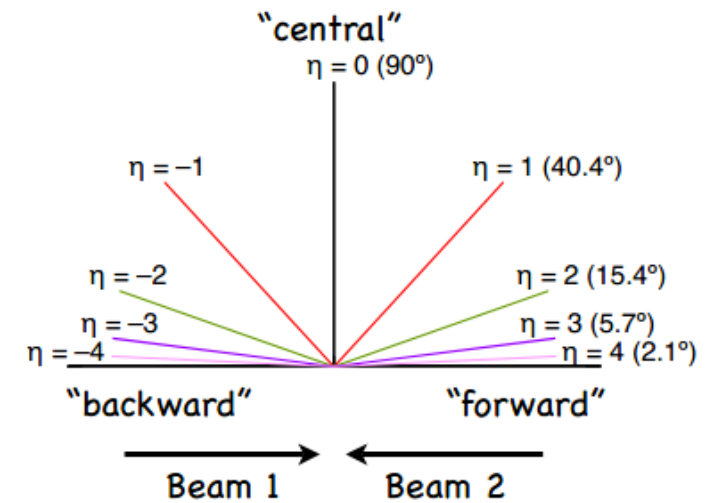
$$y \equiv \frac{1}{2} \ln\left(\frac{E + p_z}{E - p_z}\right)$$

$$y \approx \eta, \quad p \gg m, \quad \theta \gg 1/\gamma$$

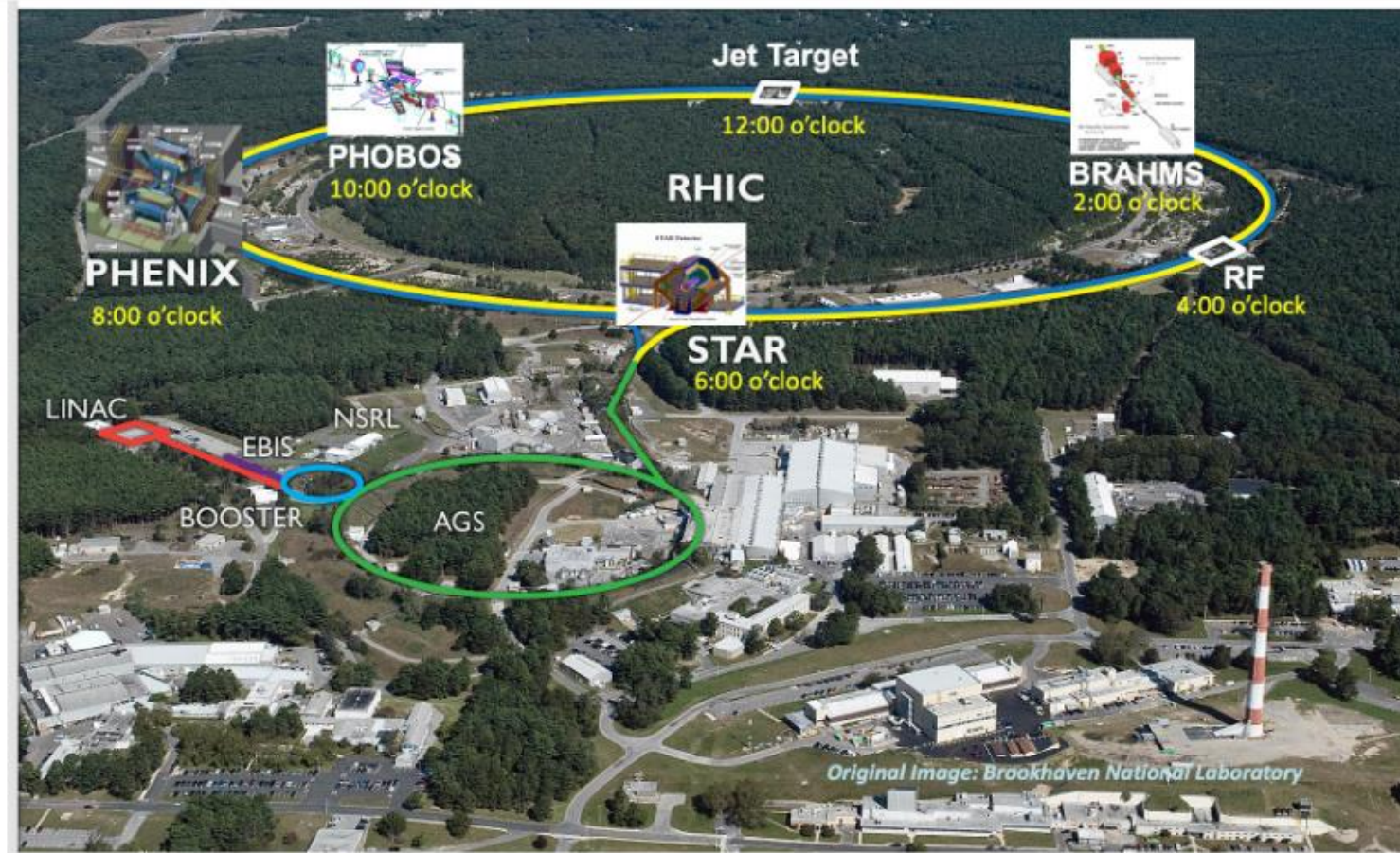
- Rapidity is invariant under Lorentz boosts in z
- *Azimuthal angle*,  $\varphi$ , is defined in x-y plane

## Collision centrality

- Peripheral collision
  - Large distance between centers of nuclei
  - Small number of **nucleons-participants**
  - **Small multiplicity of created particles**
- Central collision
  - Small distance between centers of nuclei
  - Large number of **nucleons-participants**
  - **Large particle multiplicity**



# Relativistic Heavy Ion Collider (RHIC)



## ➤ The most versatile particle collider

- ✓ The only polarized proton collider in the world
- ✓ Type of collisions:  $p+p$ ,  $p+Au$ ,  $d+Au$ ,  $Cu+Au$ ,  $Cu+Cu$ ,  $Ru+Ru$ ,  $Zr+Zr$ ,  $Au+Au$ ,  $U+U$ ,...
- ✓ Center-of-mass energy for  $Au+Au$  collisions: 3.0 - 7.7 - 200 GeV

Fixed-Target mode Collider mode

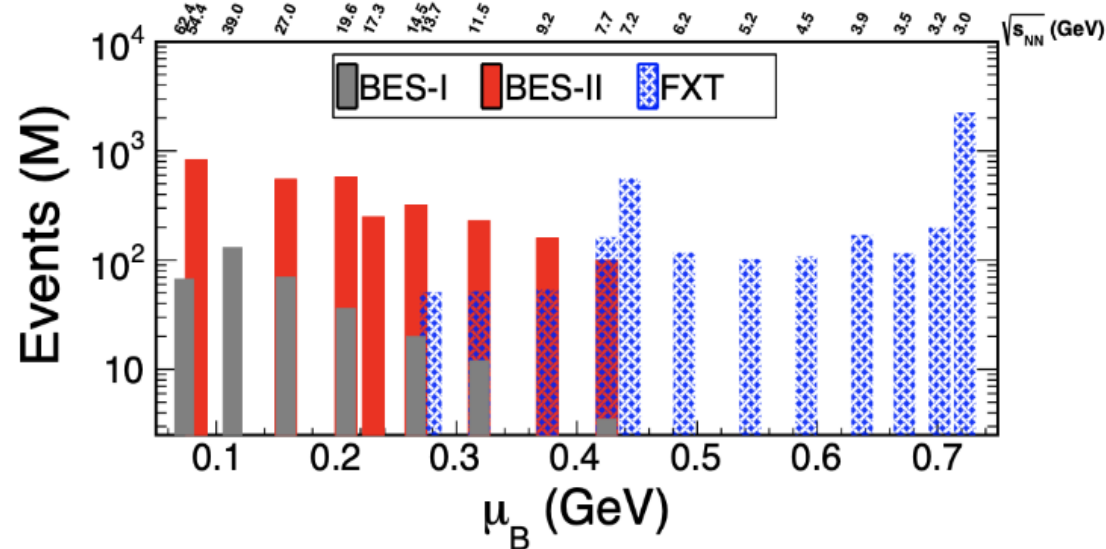
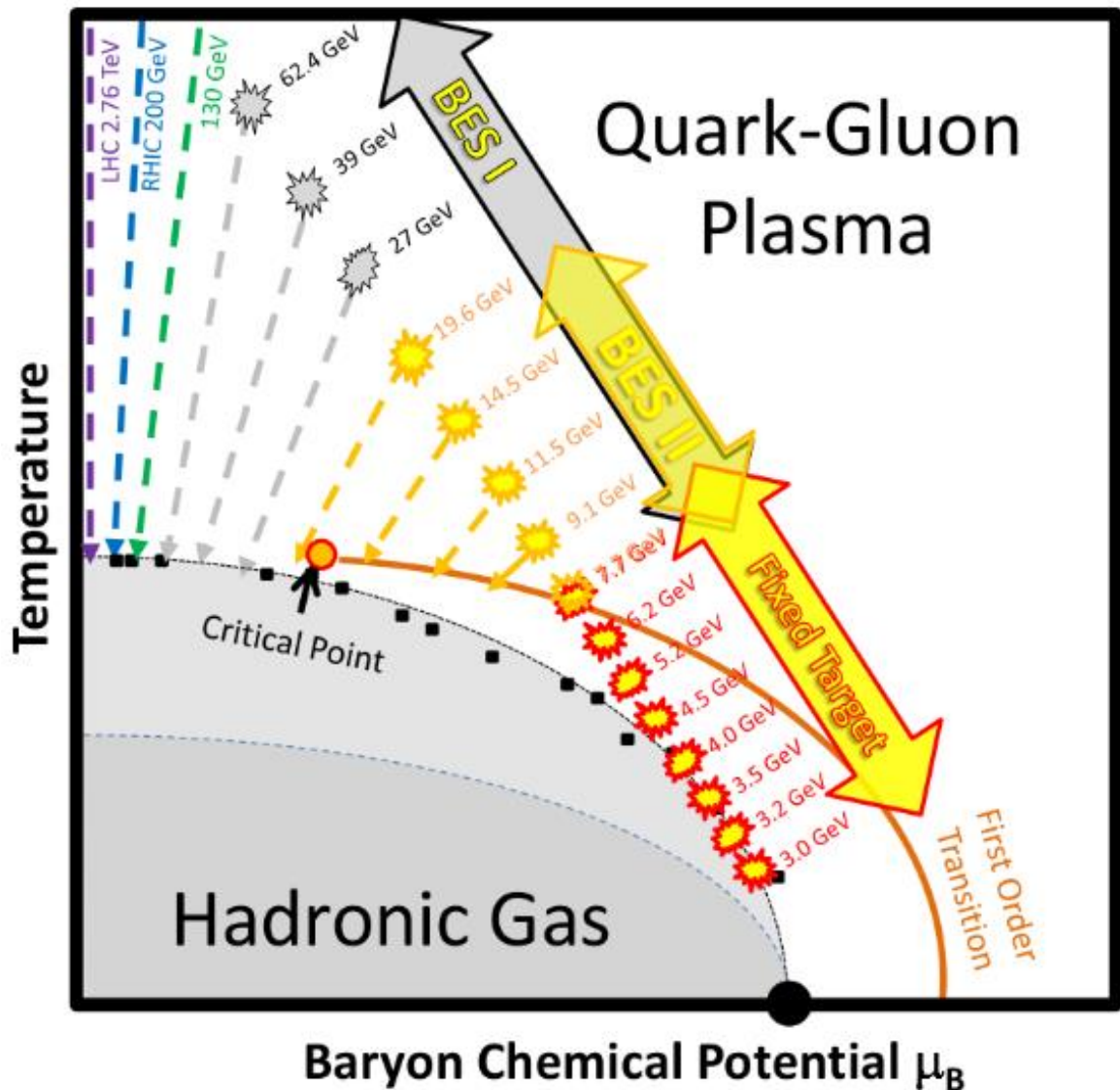
# STAR ☆ BES-I → BES-II and FXT

BES-I:

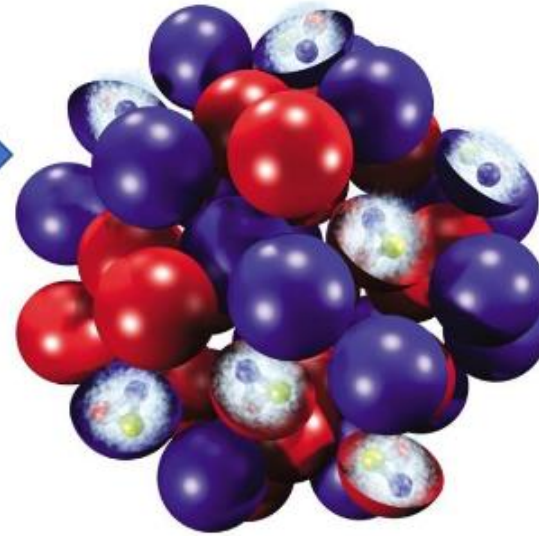
- Search for the QGP turn-off signatures
- Search for the first-order phase transition
- Search for the critical point

BES-II and fixed-target (FXT) program:

- Need higher statistics ( $\geq 10$  times than in BES-I) for precise measurements
- Detector upgrades (increased acceptance and PID capabilities)
- Access to energies  $\sqrt{s_{NN}} < 7.7$  GeV via FXT

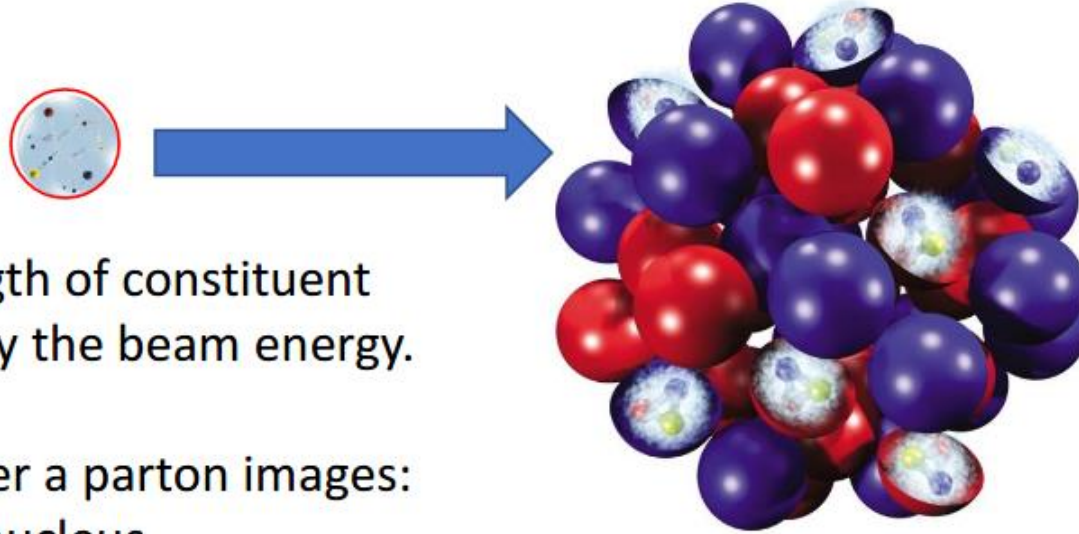


# How Does the Nucleus Look Like?



- deBroglie wavelength of constituent partons is effected by the beam energy.
- Determines whether a parton images:
  - A. The whole nucleus
  - B. Individual nucleons
  - C. Individual partons

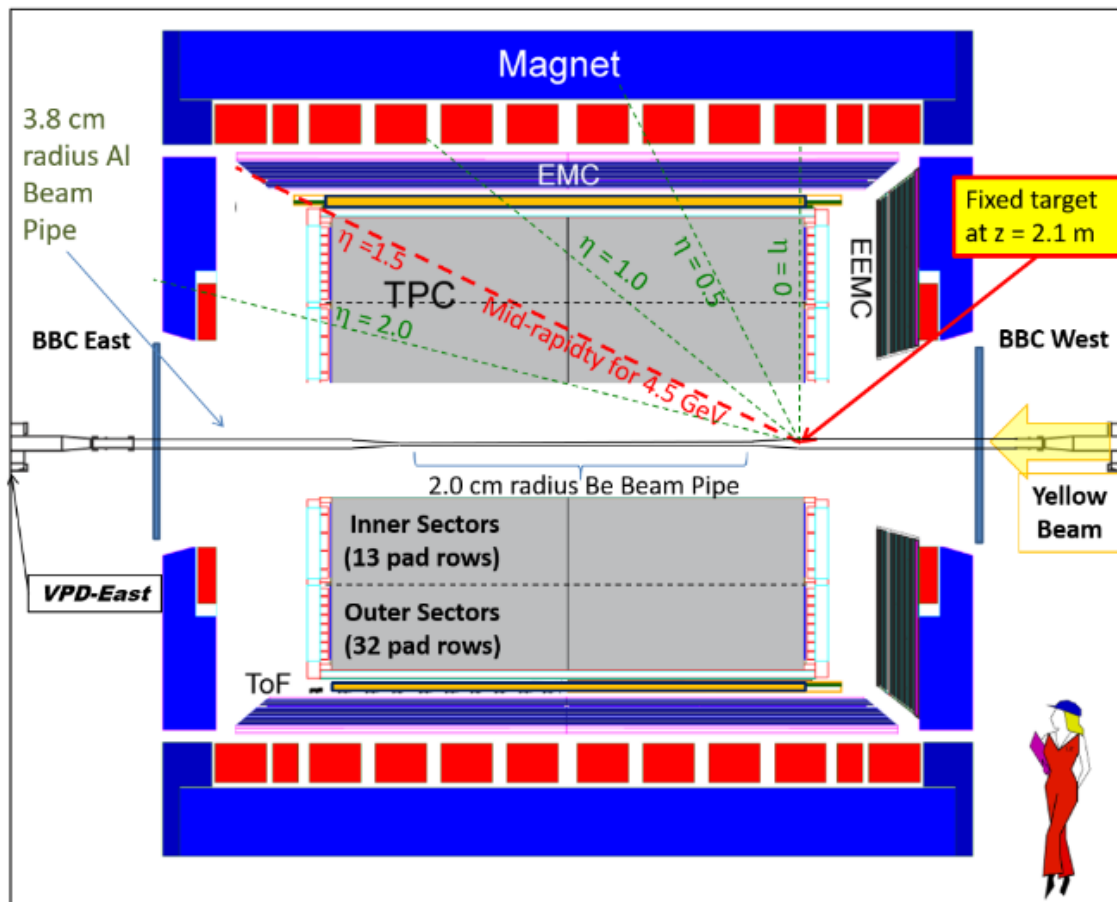
# How Does the Nucleus Look Like?



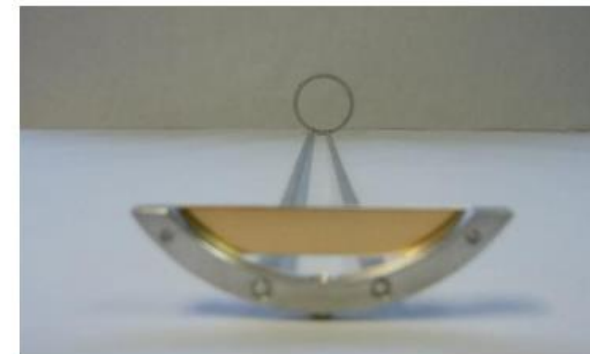
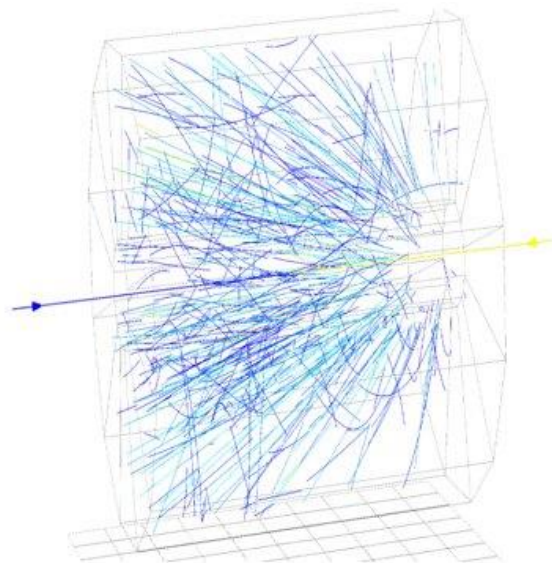
- deBroglie wavelength of constituent partons is effected by the beam energy.
- Determines whether a parton images:
  - A. The whole nucleus
  - B. Individual nucleons
  - C. Individual partons

At lower energy, nucleons are opaque, and the valence quarks are stopped in the fireball.  
Excess quarks  $\rightarrow$  higher  $\mu_B$

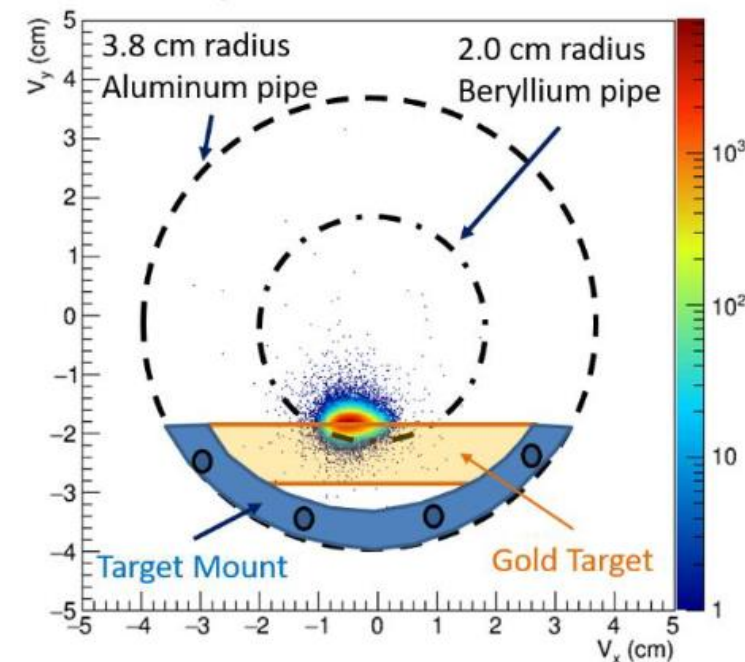
At higher energy, nucleons are transparent, and the valence quarks are pass through and exit the fireball.  
Equal quarks and anti-quarks  $\rightarrow$  lower  $\mu_B$



$$\eta = \frac{1}{2} \ln \left( \frac{|\mathbf{p}| + p_L}{|\mathbf{p}| - p_L} \right)$$



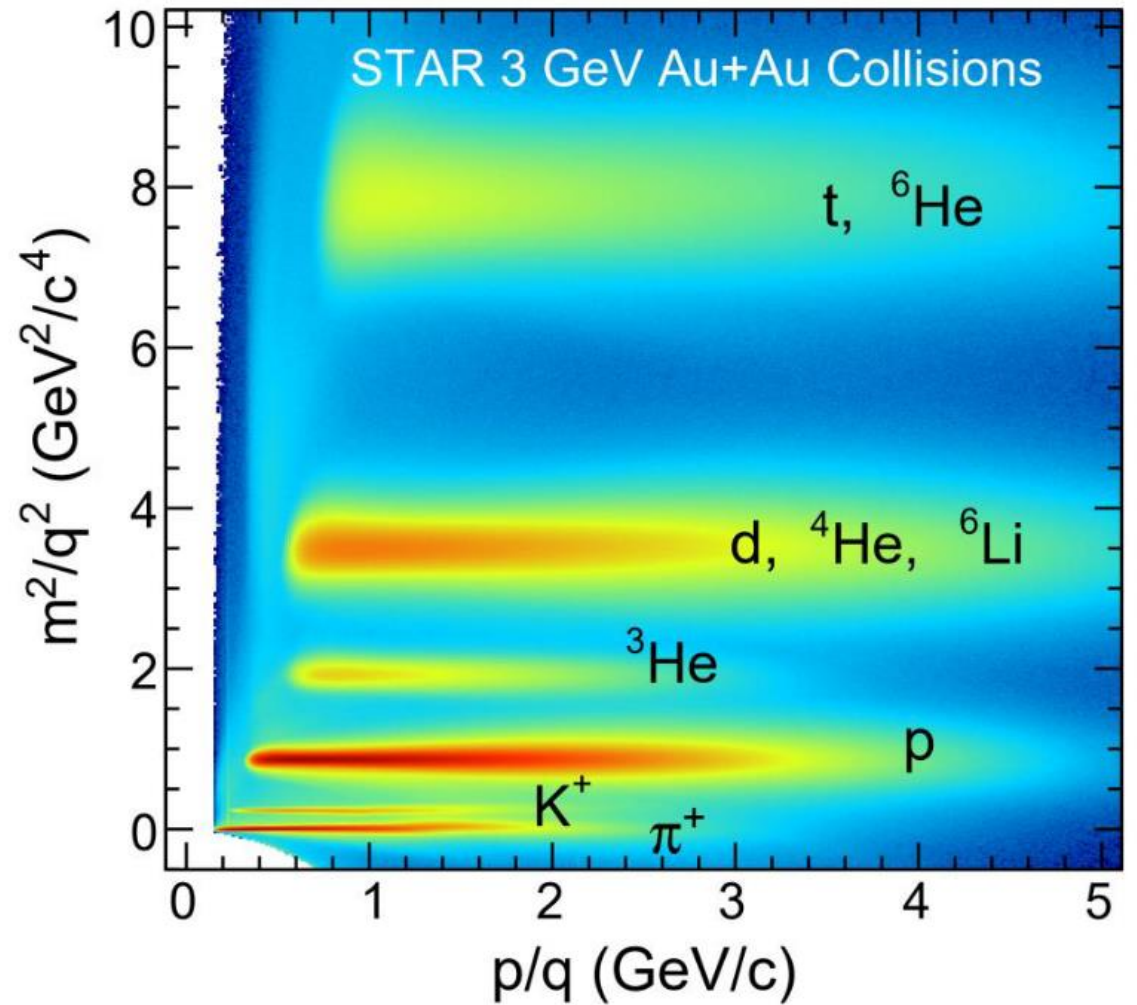
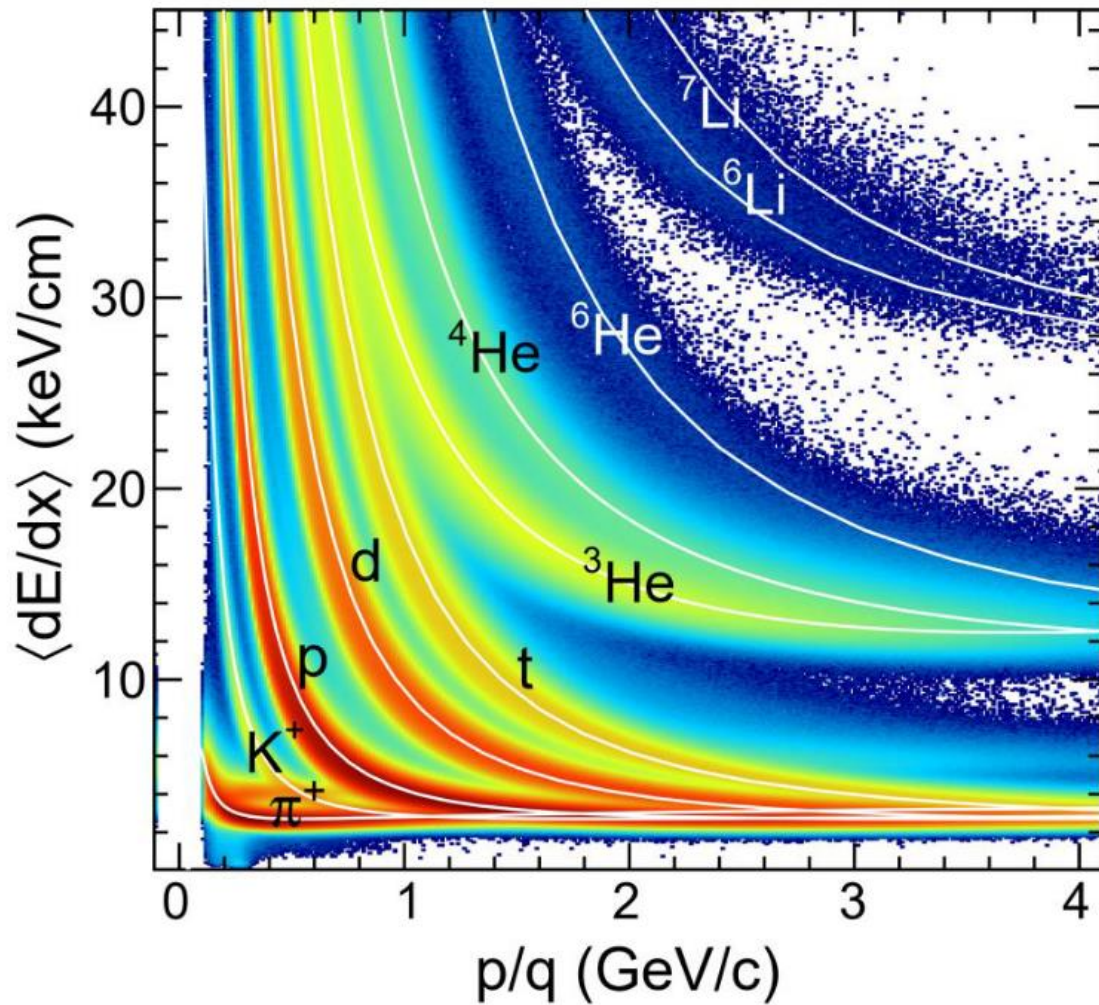
$V_y$  vs.  $V_x$  Distribution



Gold target:

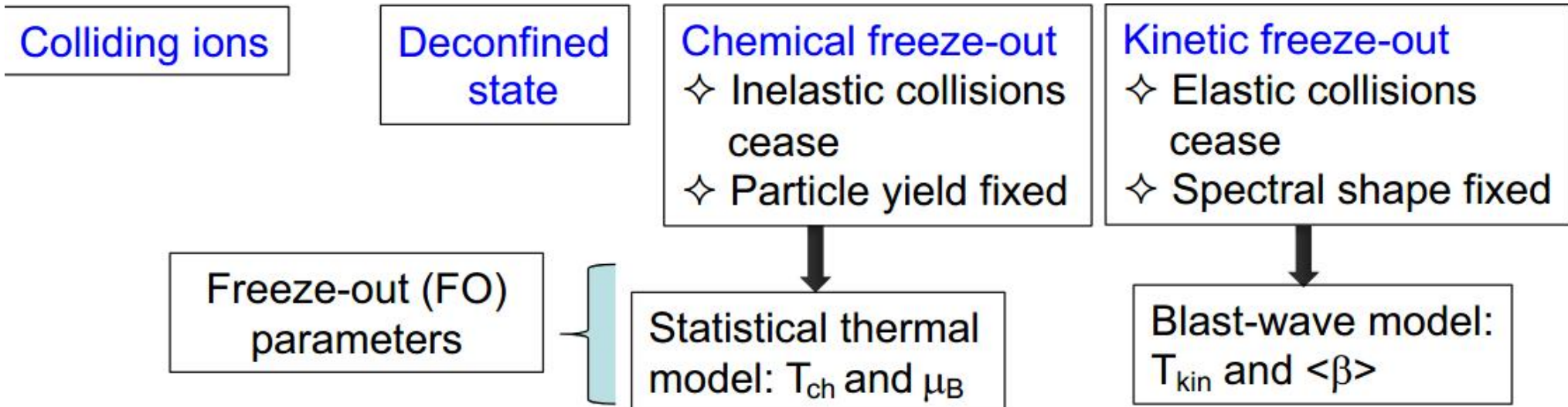
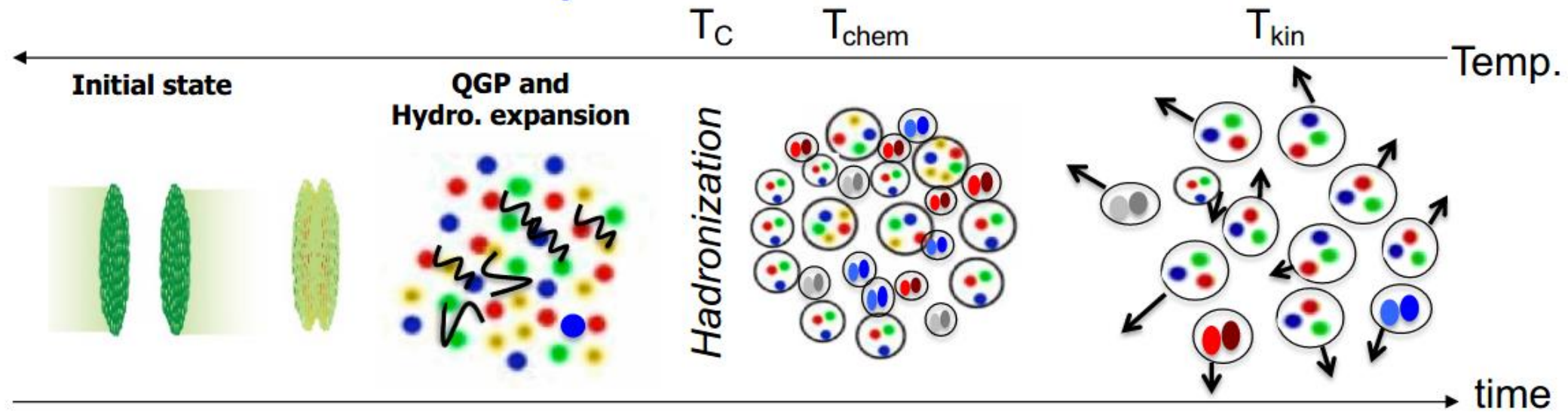
- 2 cm below nominal beam axis
- 2 m from center of STAR
- 250  $\mu\text{m}$  foil

# STAR ☆ Particle Identification at STAR



**Good particle identification in a broad momentum range using TPC and TOF**

# Evolution of the High-Energy Heavy-Ion Collision

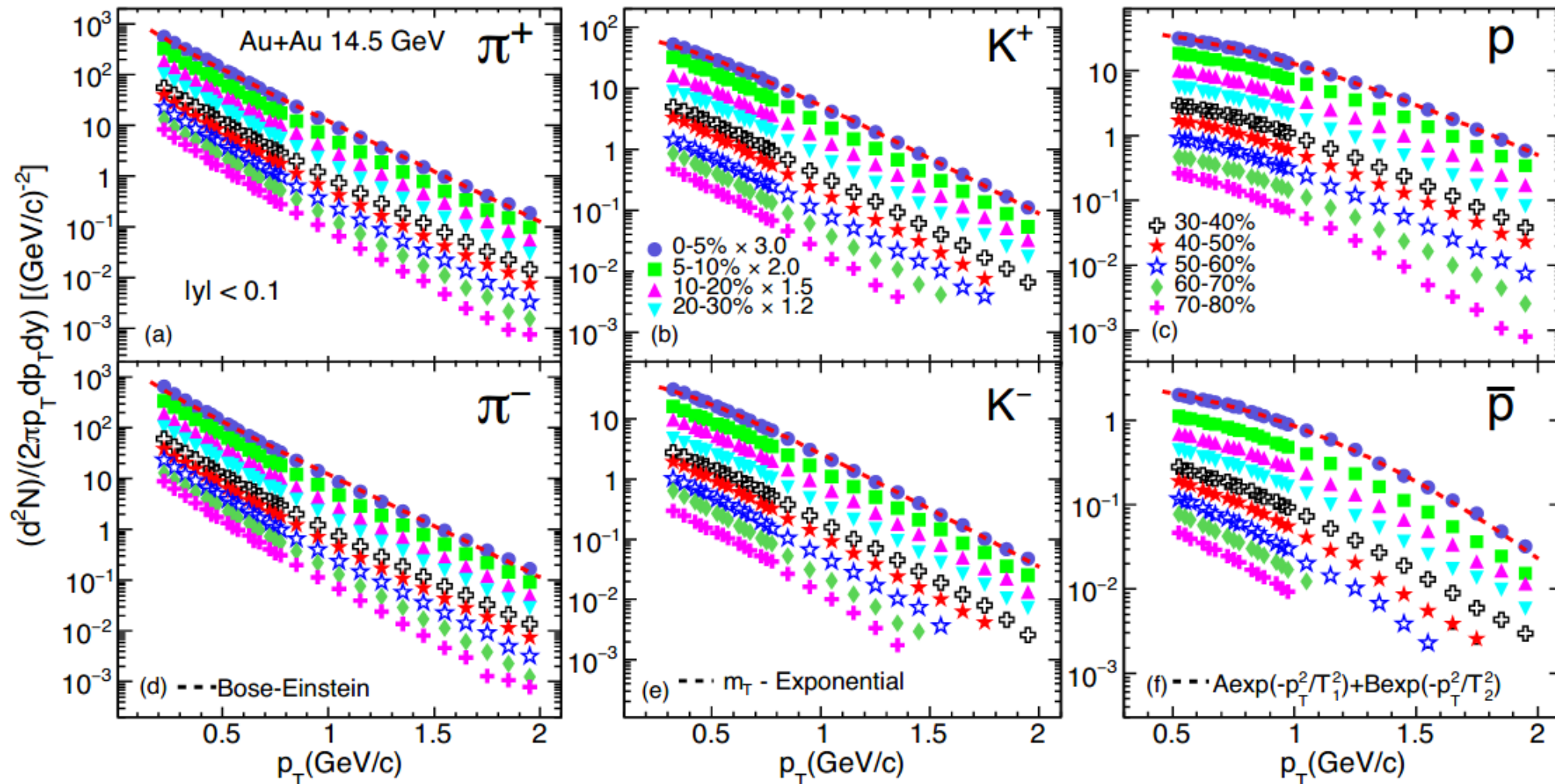


**Particle Yields and Ratios:** provide Information about QCD phase diagram

# Transverse Momentum Spectra

**Au+Au @ 14.5 GeV**

STAR. Phys. Rev. C 101, 024905 (2020)



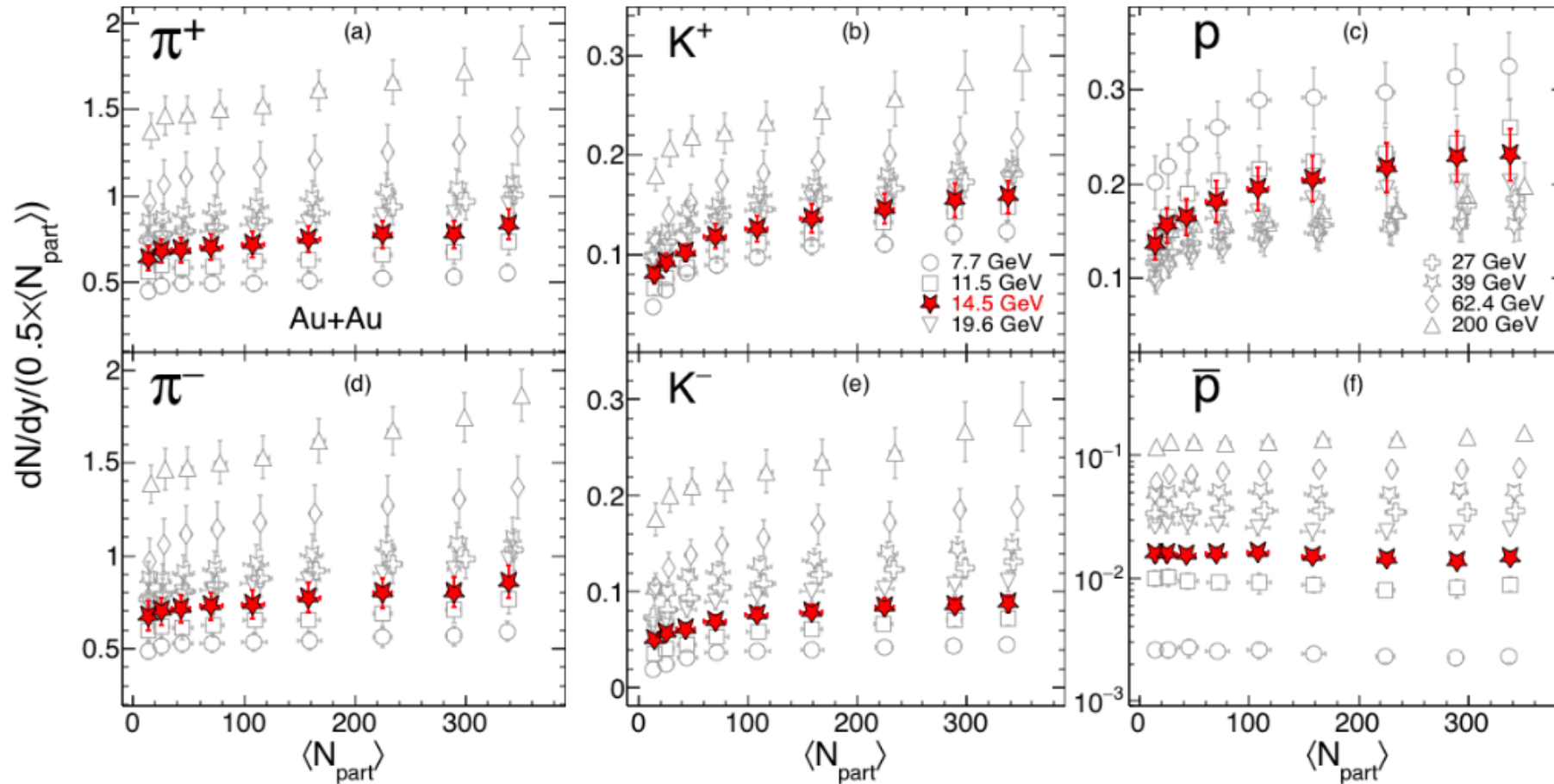
Integrating over full  $p_T$  range gives particle yield ( $dN/dy$ )

# Particle Yields

STAR: PRC **96**, 044904 (2017)

**Au+Au @ 14.5 GeV**

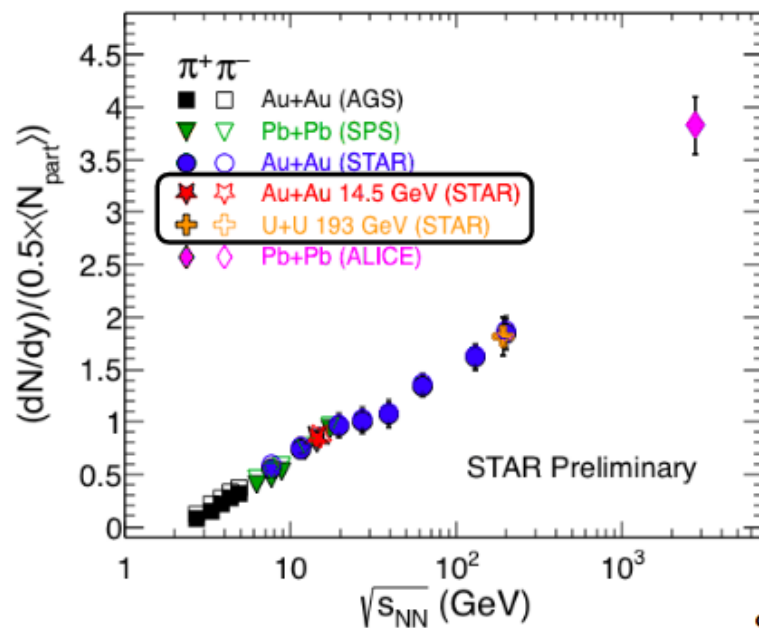
STAR. Phys. Rev. C 101, 024905 (2020)



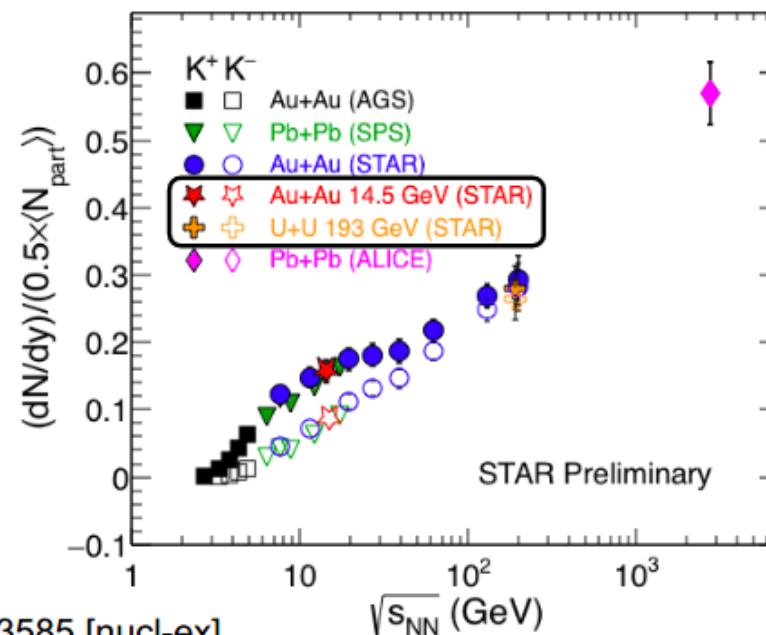
Yields @  
14.5 GeV:

- Increase from peripheral to central collisions (except for  $\bar{p}$ )
- Fall in the energy dependence trend

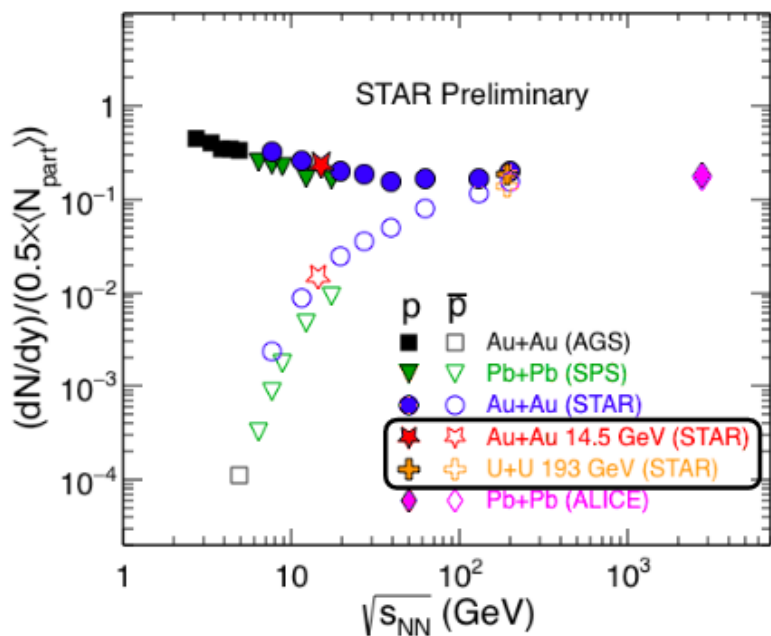
# Energy Dependence of Particle Yields



STAR: PRC 96,  
044904 (2017)



STAR: arXiv:1908.03585 [nucl-ex]

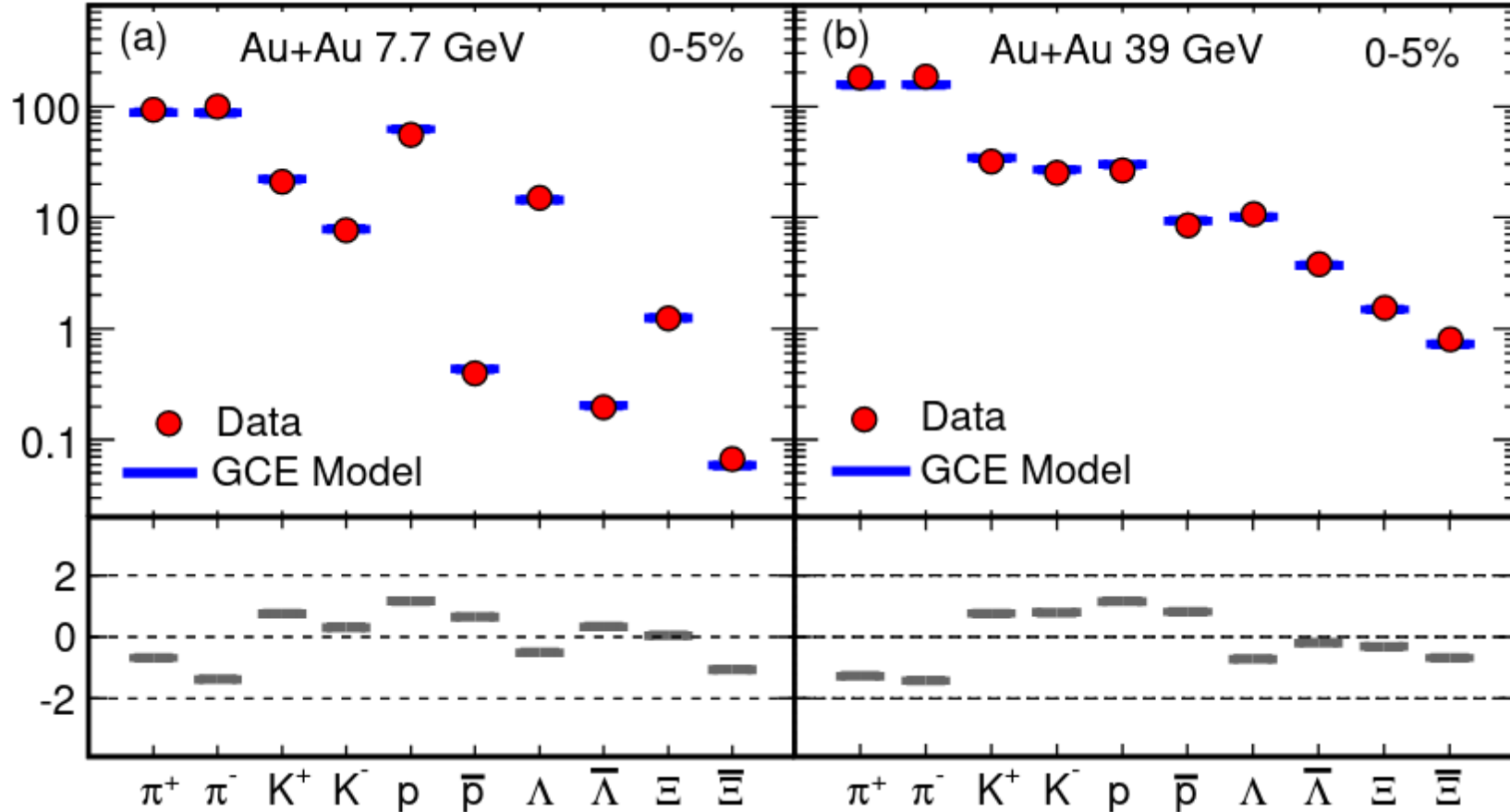


- Yields increase as a function of collision energy except for protons
- Au+Au 14.5 GeV and U+U 193 GeV fit well in the trend*
- Higher energies:** Similar (pair) production of particle and anti-particle

**Lower energies:**  $\pi^- > \pi^+, K^+ > K^-, p > \bar{p}$

# Extracting Baryon Chemical Potential and Temperature at Chemical Freeze-Out

STAR. Phys. Rev. C 96, 044904 (2017)



Considering the grand canonical case, for a hadron gas of volume  $V$  and temperature  $T$ , the logarithm of the total partition function is given by [50],

$$\ln Z^{GC}(T, V, \{\mu_i\}) = \sum_{\text{species } i} \frac{g_i V}{(2\pi)^3} \int d^3p \ln(1 \pm e^{-\beta(E_i - \mu_i)})^{\pm 1} \quad (7)$$

where,  $g_i$  and  $\mu_i$  are degeneracy and chemical potential of hadron species  $i$  respectively,  $\beta = 1/T$ , and  $E_i = \sqrt{p^2 + m_i^2}$ ,  $m_i$  being the mass of particle. The plus sign corresponds to fermions and minus sign to bosons. The chemical potential for particle species  $i$  in this case is given by

$$\mu_i = B_i \mu_B + Q_i \mu_Q + S_i \mu_S, \quad (8)$$

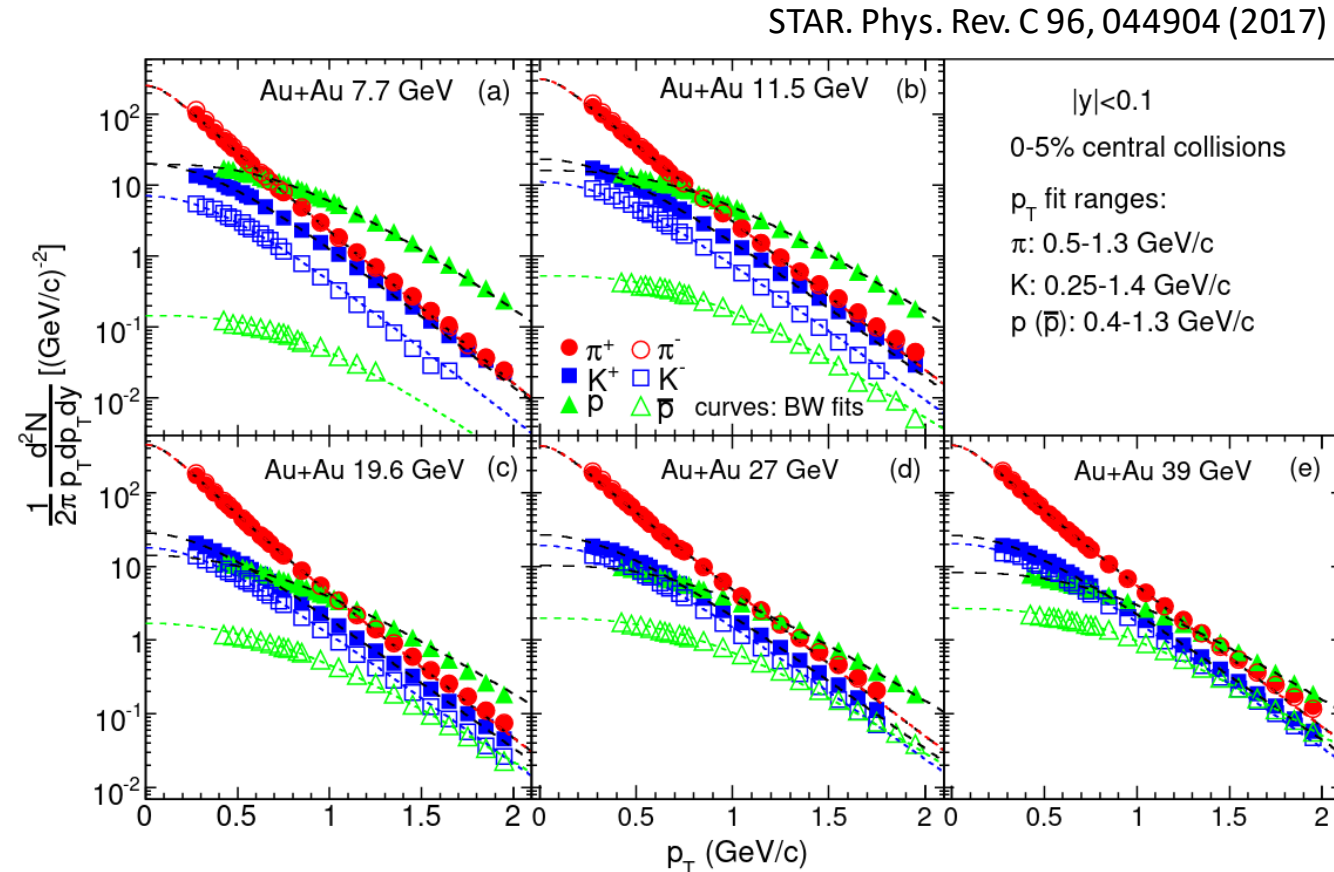
where  $B_i$ ,  $S_i$ , and  $Q_i$  are the baryon number, strangeness, and charge number, respectively, of hadron species  $i$ , and  $\mu_B$ ,  $\mu_Q$ , and  $\mu_S$  are the respective chemical potentials.

# Extracting Parameters of the Quark-Gluon Matter at Kinetic Freeze-Out

- The kinetic freeze-out parameters are obtained by fitting the spectra with a blast wave model. The model assumes that the particles are locally thermalized at a kinetic freeze-out temperature and are moving with a common transverse collective flow velocity. Assuming a radially boosted thermal source, with a kinetic freeze-out temperature  $T_{\text{kin}}$  and a transverse radial flow velocity  $\beta$ , the  $p_T$  distribution of the particles is given by

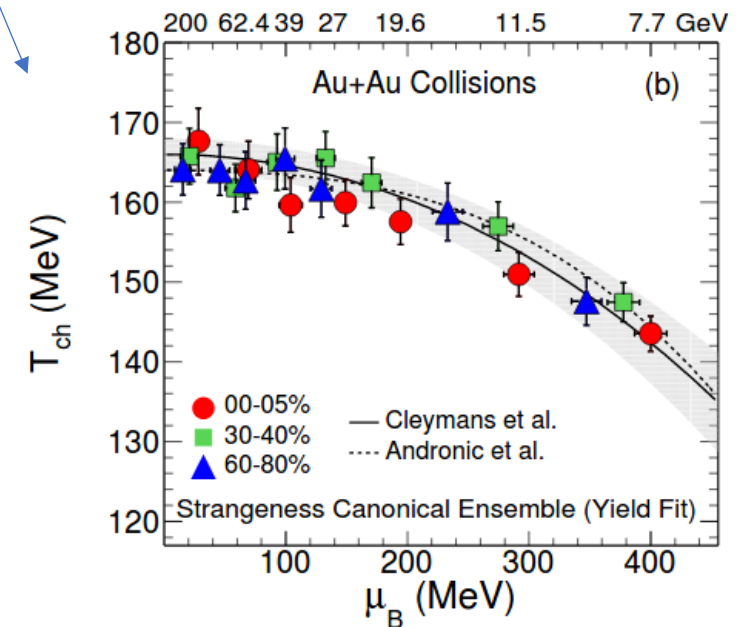
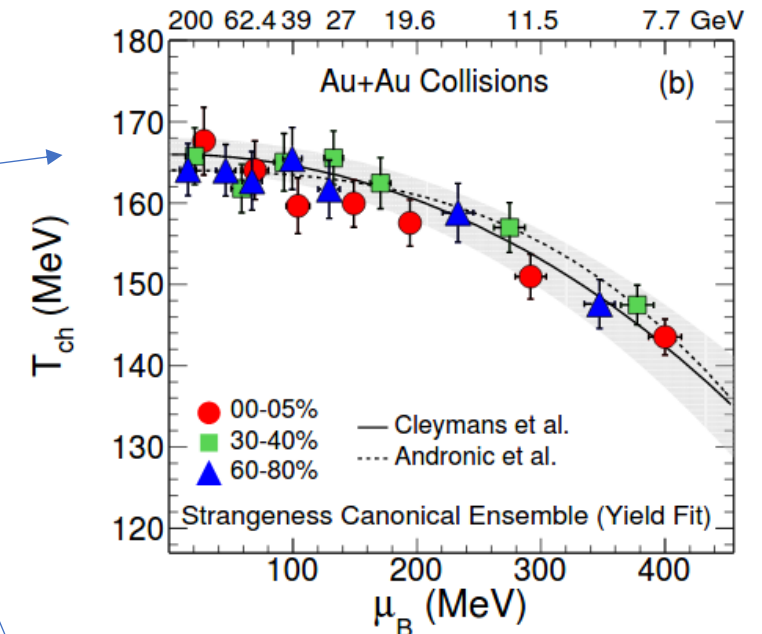
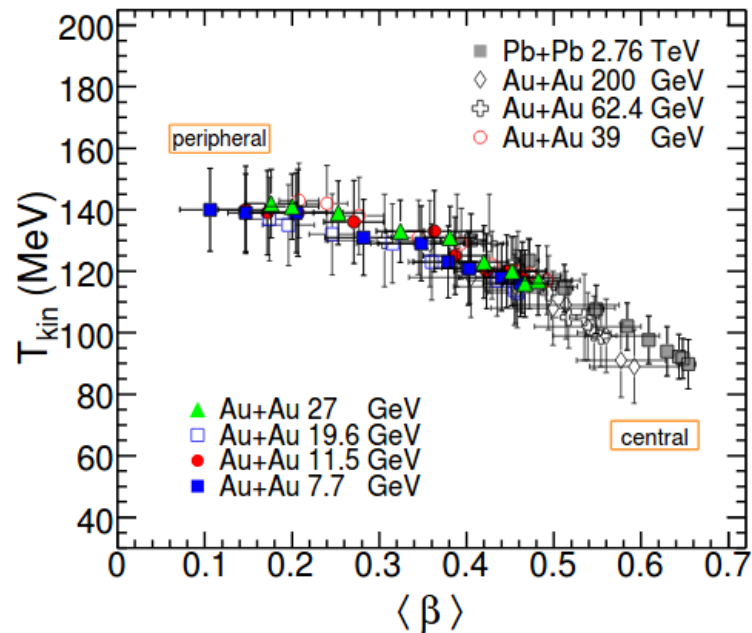
$$\frac{dN}{p_T dp_T} \propto \int_0^R r dr m_T I_0 \left( \frac{p_T \sinh \rho(r)}{T_{\text{kin}}} \right) \times K_1 \left( \frac{m_T \cosh \rho(r)}{T_{\text{kin}}} \right)$$

where  $m_T$  is the transverse mass of a hadron,  $\rho(r) = \tanh^{-1}\beta$ , and  $I_0$  and  $K_1$  are the modified Bessel functions.

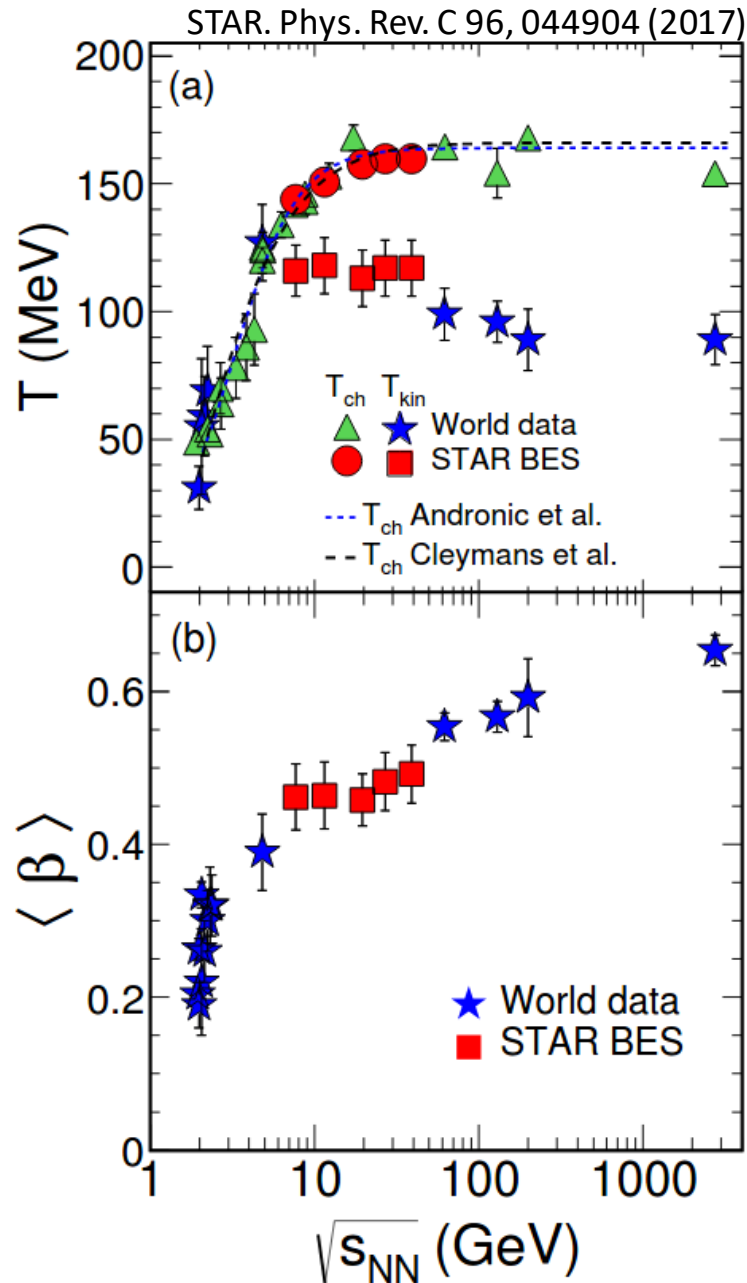


# Mapping QCD Phase Diagram

- Using a statistical equilibrium model and the measured particle yields, one can estimate the location of the phase diagram
- The  $\langle \beta \rangle$  decreases from central to peripheral collisions indicating more rapid expansion in central collisions
- $T_{\text{kin}}$  increases from central to peripheral collisions, consistent with the expectation of a shorter-lived fireball in peripheral collisions

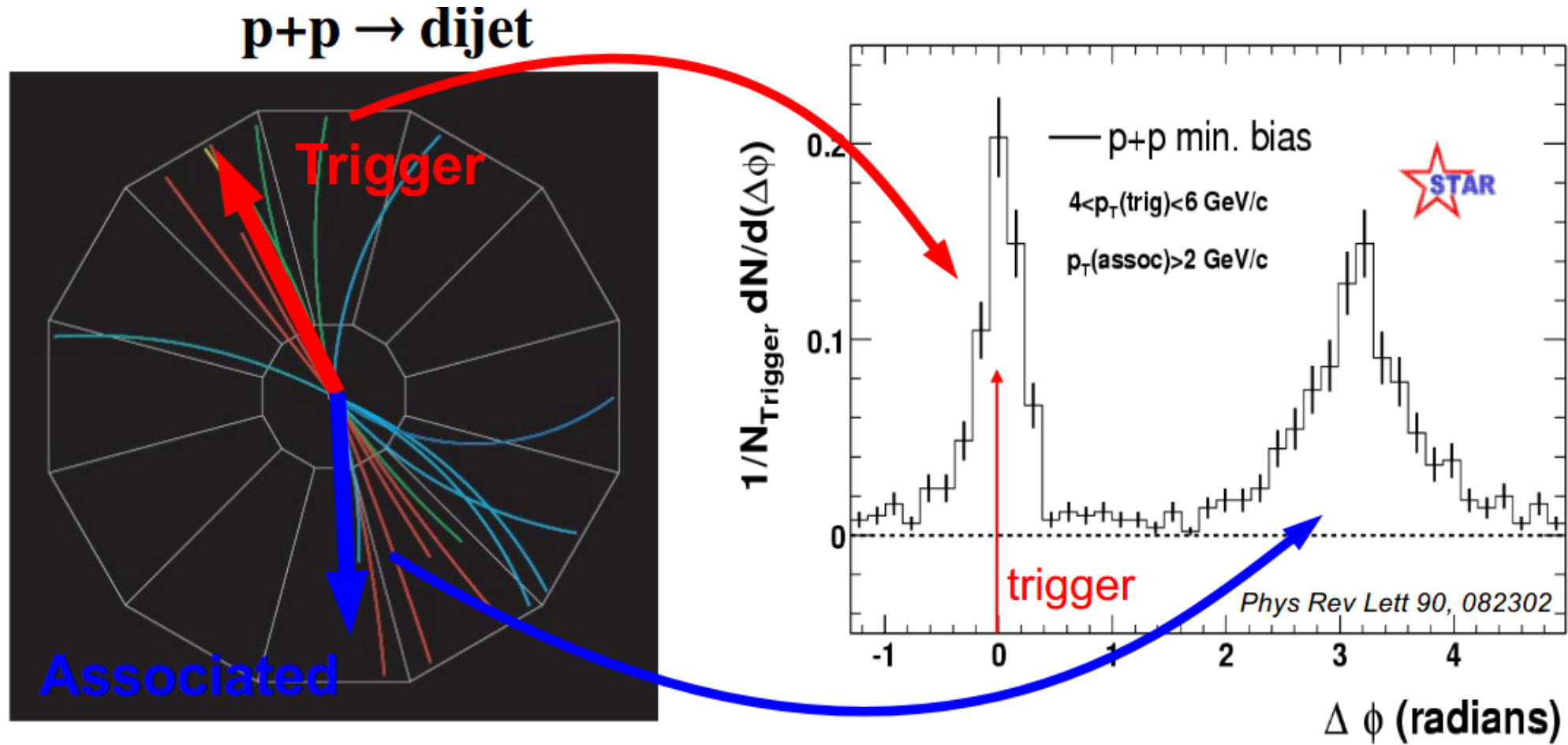


# Energy Dependence of Freeze-out Parameters



- Chemical freeze-out temperature increases and then saturates with beam energy
- Kinetic freeze-out temperature decreases while  $\langle \beta \rangle$  (collectivity) increases with beam energy for central collisions
- Difference between chemical and kinetic freeze-out temperatures increases with beam energy
  - Suggests system interacts for longer duration at higher collisions energies

# QGP at High Collision Energies



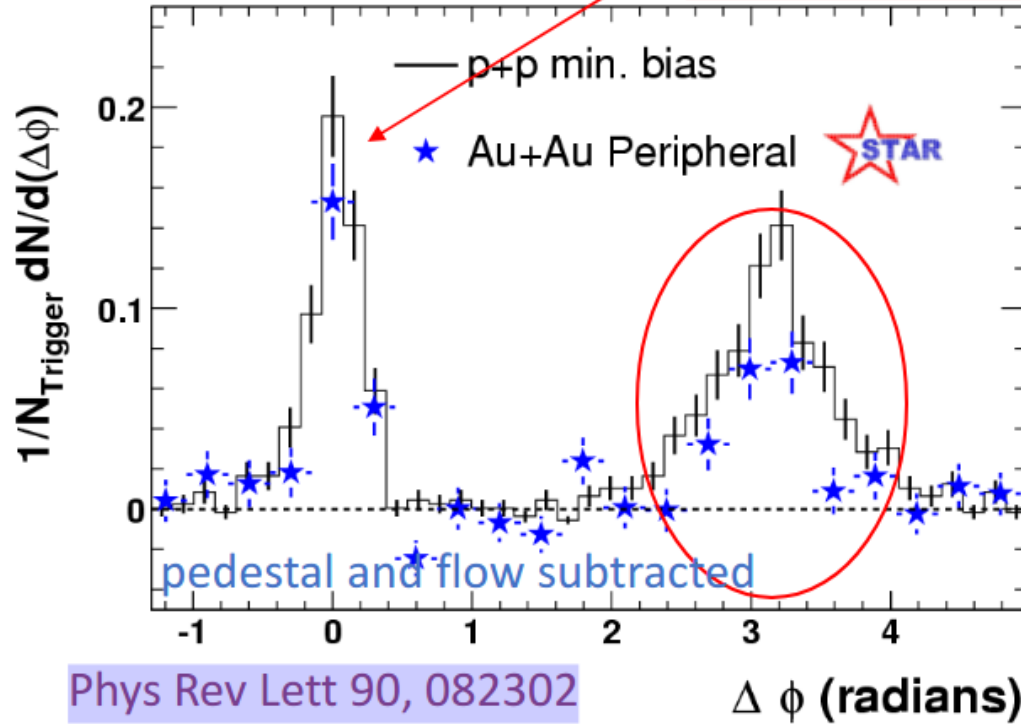
Select high momentum particles → biased towards jets

# QGP at High Collision Energies

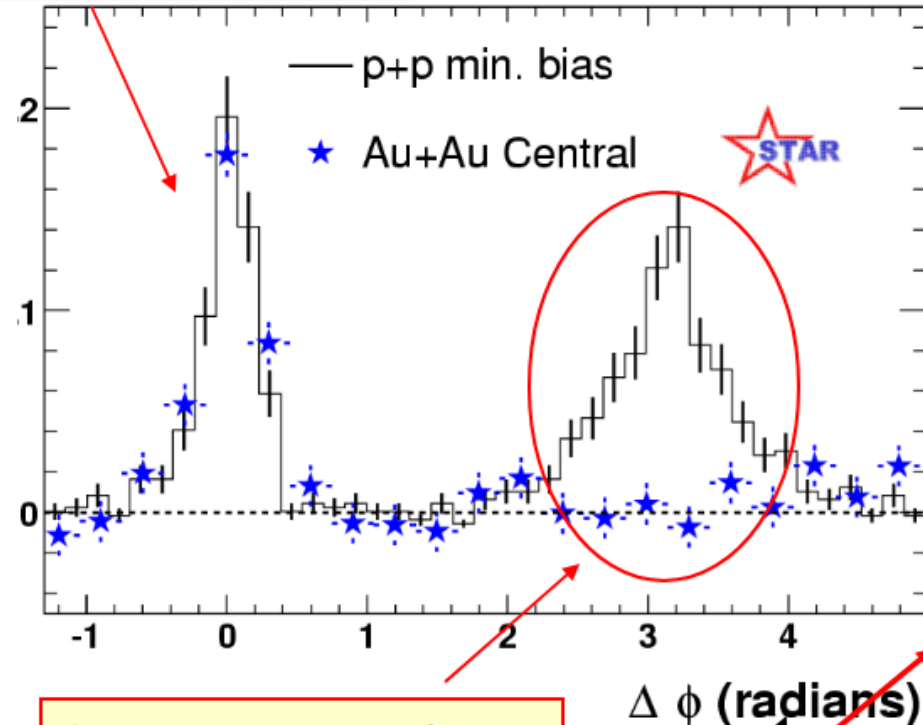
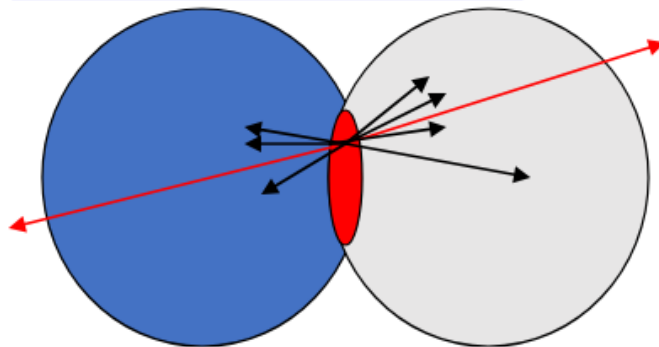
Au+Au peripheral

Near-side: peripheral and central Au+Au similar to p+p

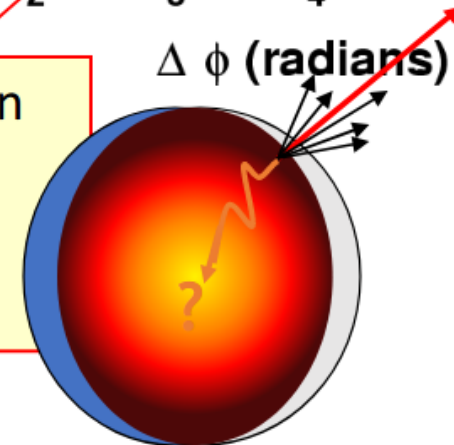
Au+Au central



Phys Rev Lett 90, 082302



Strong suppression of back-to-back correlations in central Au+Au



# Identifying QGP at High-Energy Collisions

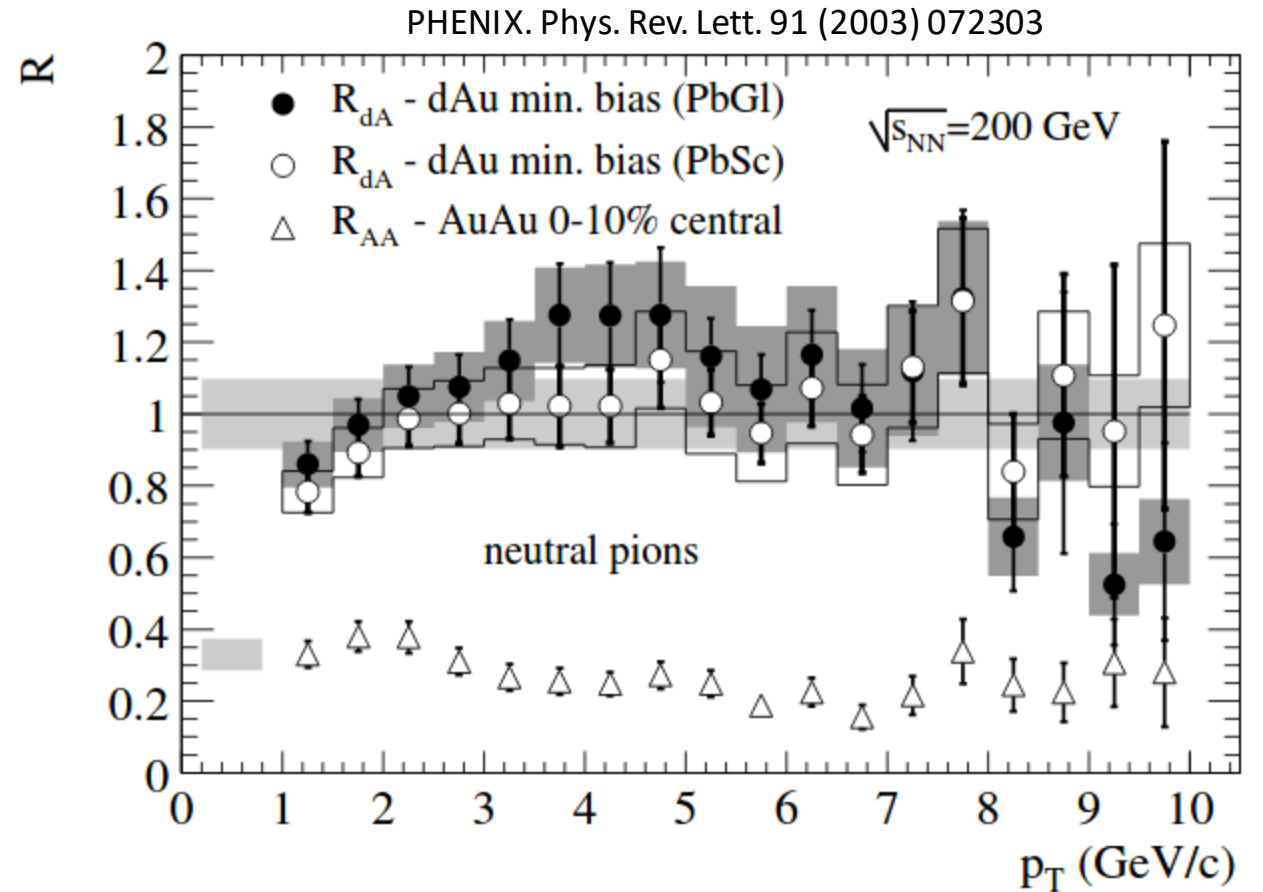
$$R_{AA} = \frac{1}{N_{coll}} \times \frac{Y_{AA}}{Y_{pp}}$$

Superposition of NN collisions  $\rightarrow R_{AA}=1$

Suppression  $\rightarrow R_{AA} < 1$

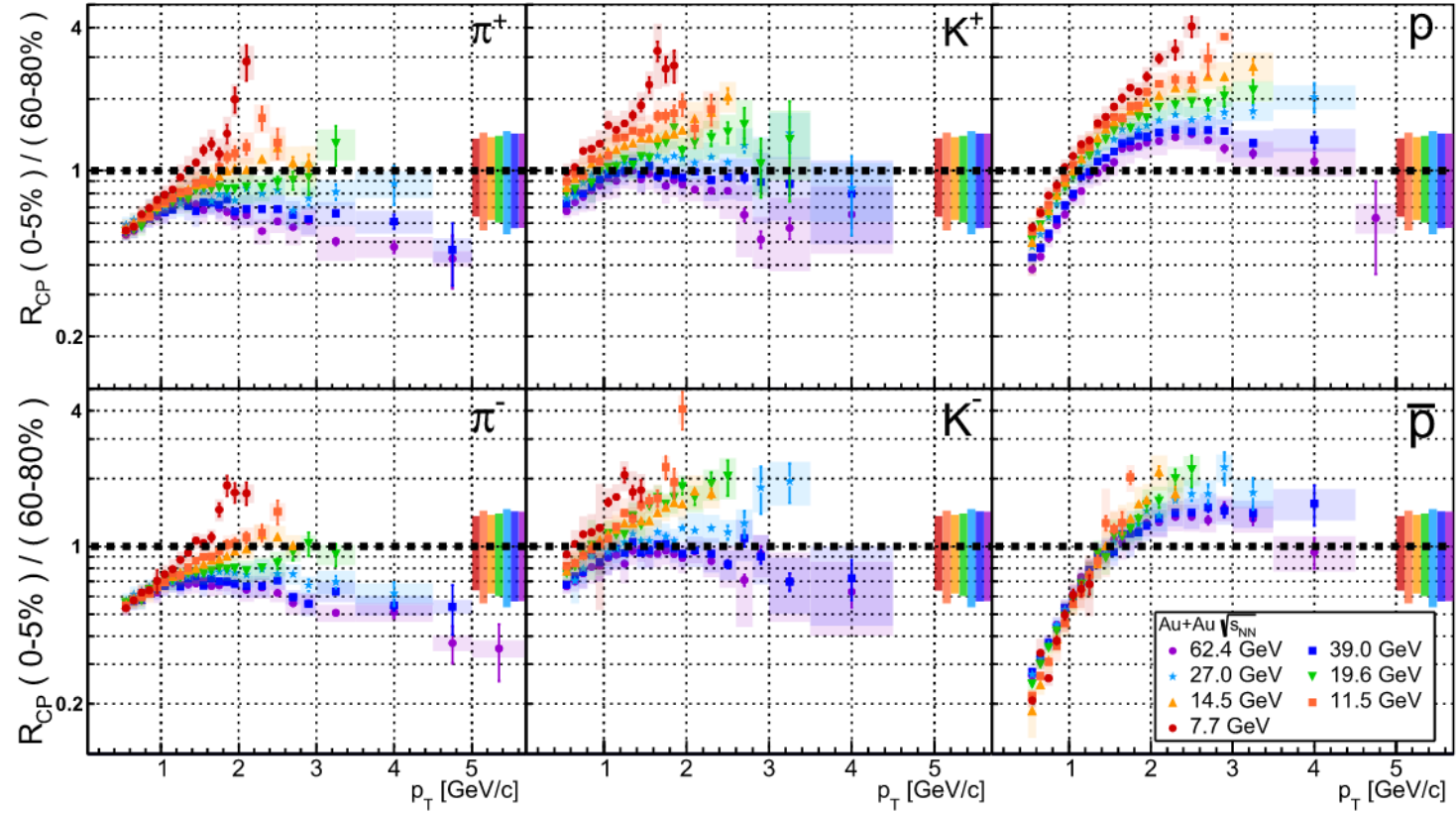
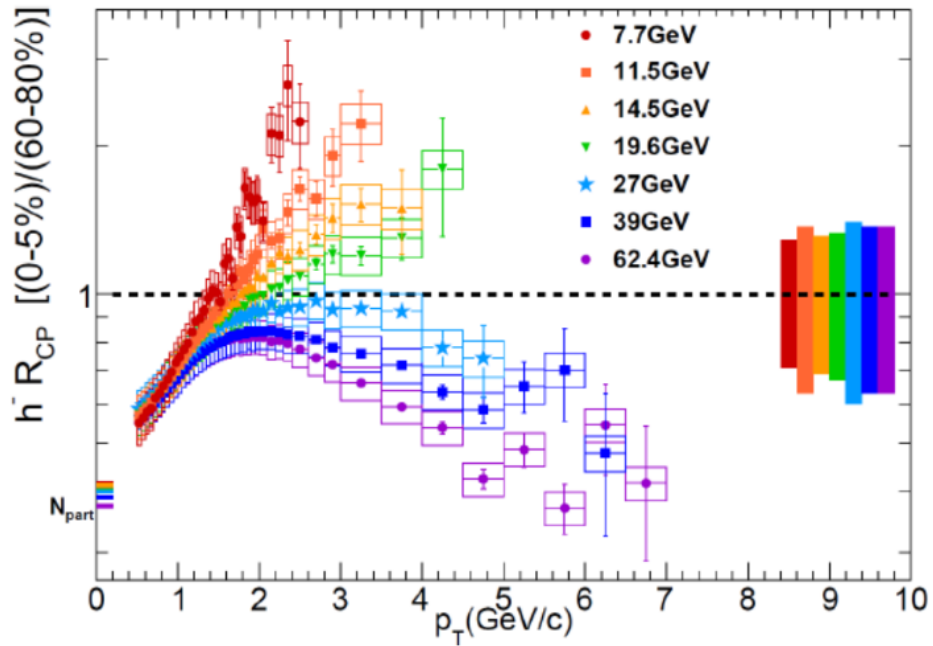
Enhancement  $\rightarrow R_{AA} > 1$

- The data clearly indicate that there is no suppression of high- $p_T$  particles in d+Au collisions.
- The data suggest, instead, that the suppression of high- $p_T$  hadrons in Au+Au is more likely a final state effect of the produced dense medium

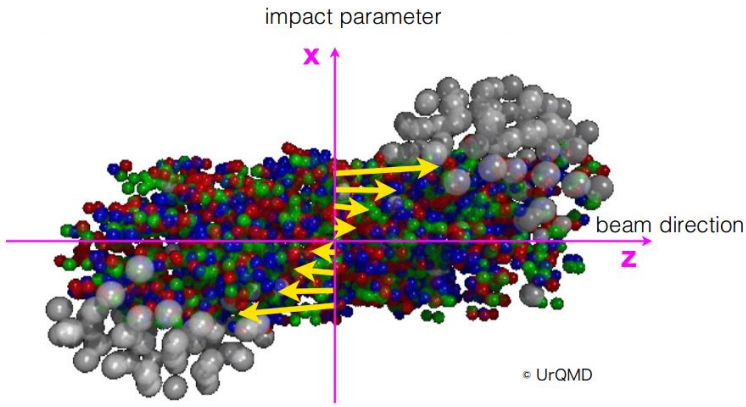


# Searching for Turn-Off Signatures of QGP

$$R_{cp} = \frac{d^2 N dp_t d\eta / \langle N_{coll} \rangle (central)}{d^2 N dp_t d\eta / \langle N_{coll} \rangle (peripheral)}$$

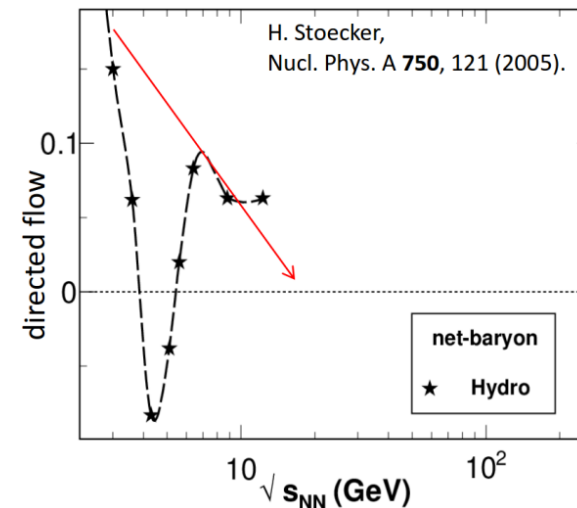
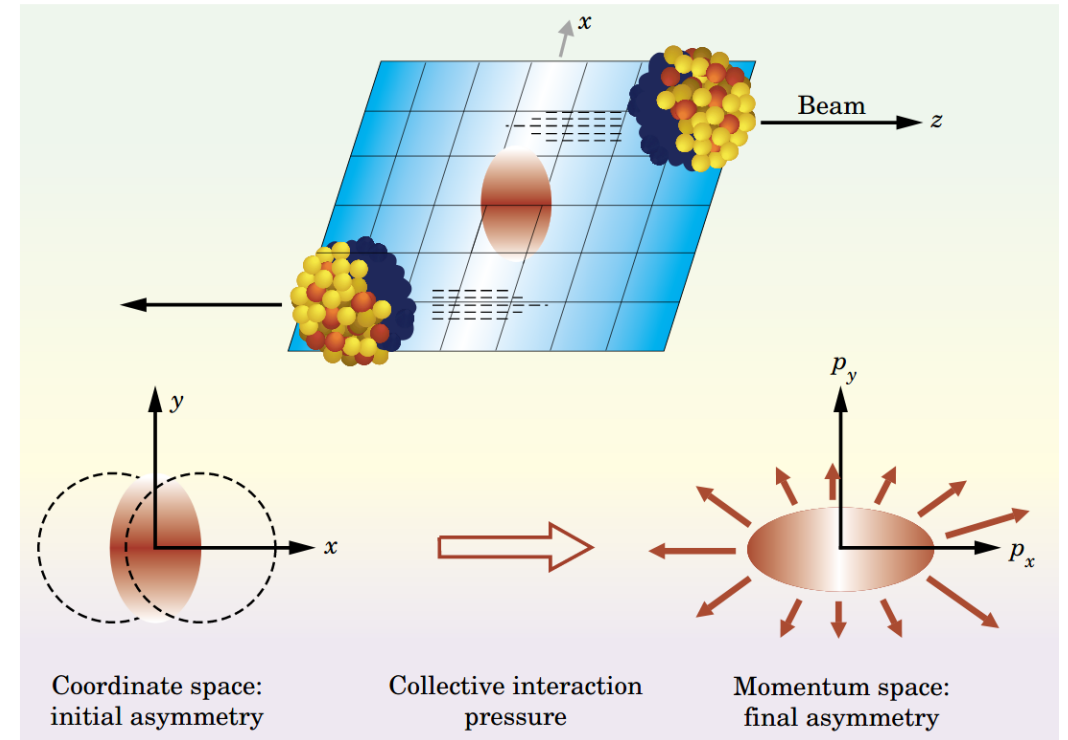


# Azimuthal Anisotropy in Heavy-Ion Collisions



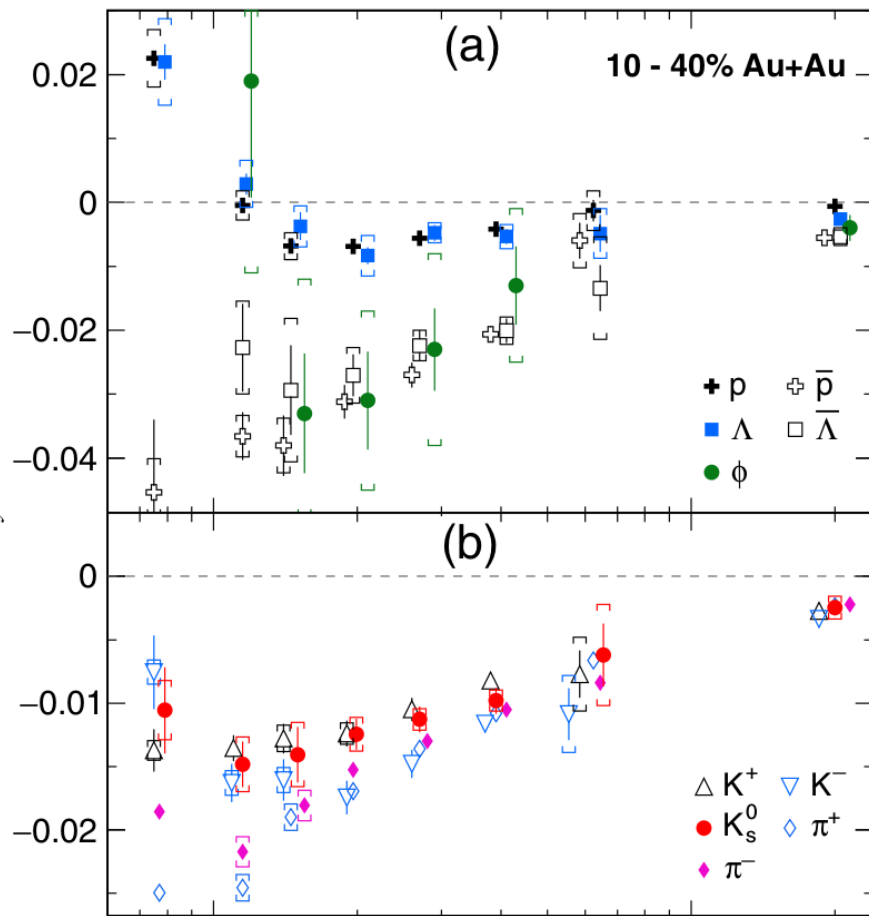
$$E \frac{d^3N}{d^3p} = \frac{1}{2\pi} \frac{d^2N}{p_t dp_t dy} \left( 1 + \sum_{n=1}^{\infty} 2v_n \cos[n(\phi - \Psi_r)] \right)$$

- $v_1 = \langle p_x / p_T \rangle$  – directed flow
  - Describes the sideward collective motion of particles within the reaction plane (x-z)
  - Probe of the softening of the EoS:
    - Strong softening: consistent with the 1st-order phase transition
    - Weaker softening: more likely due to crossover
- $v_2$  – elliptic flow
  - Sensitive to the properties of the medium



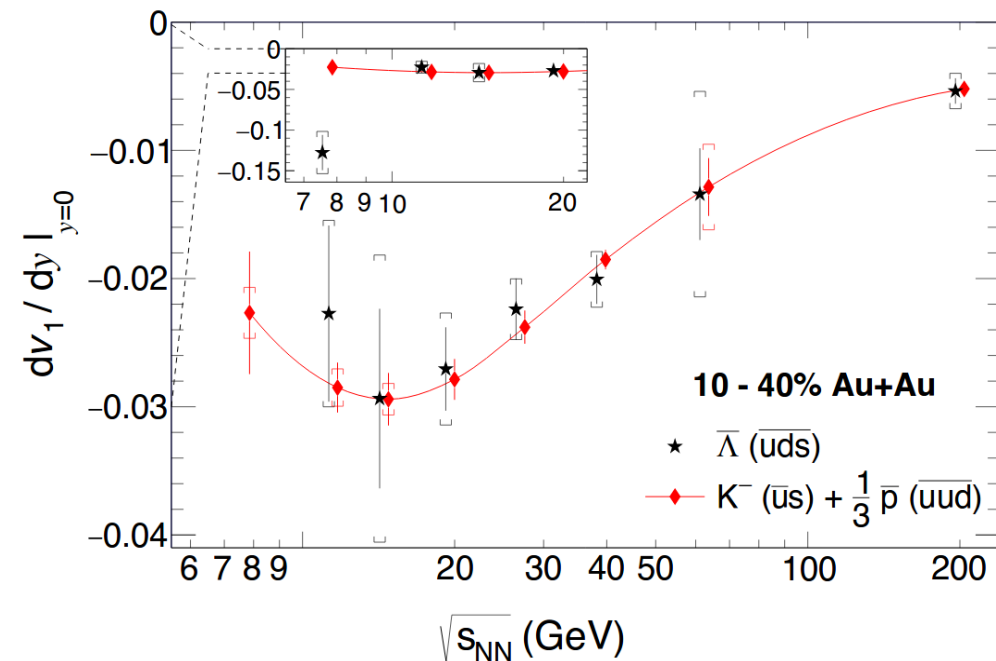
Nara, Niemi, Steinheimer, Stöcker. Phys. Lett. B 769 (2017) 543  
Ivanov, Soldatov. Phys. Rev. C 91 (2015) 024915

# Beam-Energy Dependence of Directed Flow



- $dv_1/dy$  for  $\Lambda$  and  $p$  agree within uncertainties
- $dv_1/dy$  slope for baryons changes sign in the region  $\sqrt{s_{NN}} < 14.5$  GeV
- Particles (anti- $p$ , anti- $\Lambda$ , and  $\phi$ ) with produced quarks show similar behavior for  $\sqrt{s_{NN}} > 14.5$  GeV
- Mesons show negative  $dv_1/dy$

STAR. Phys. Rev. Lett. 120 (2018) 062301

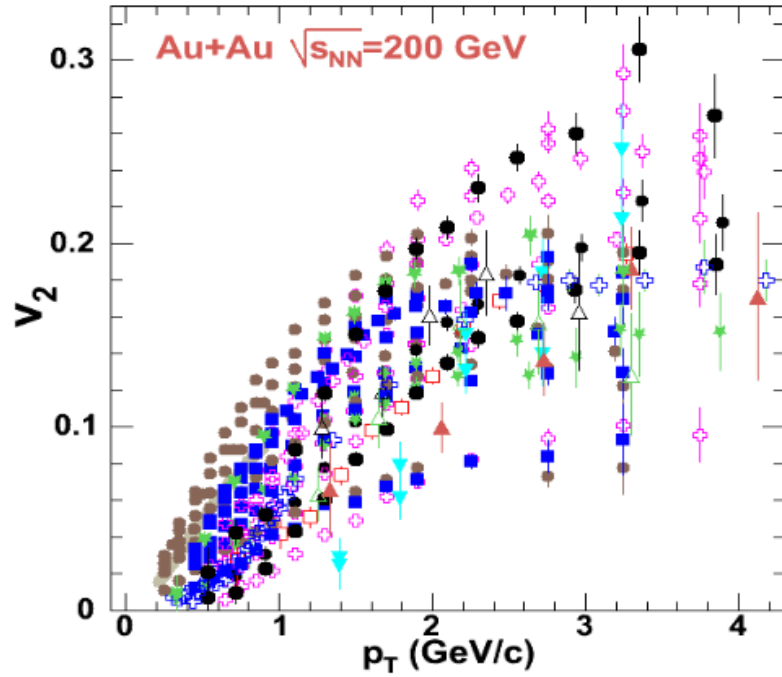


## Assumptions for coalescence sum rule:

1.  $v_1$  is developed at prehadronic stage
2. Specific types of quarks have the same  $v_1$
3. Hadrons are formed via coalescence

For anti- $\Lambda$ , prediction using coalescence sum rule agrees with measured  $v_1$  above  $\sqrt{s_{NN}} = 11.5$  GeV

# Anisotropic Flow at RHIC – scaling relations



**PHENIX** (Phys.Rev.Lett.91, Preliminary: QM05, GRC 06)

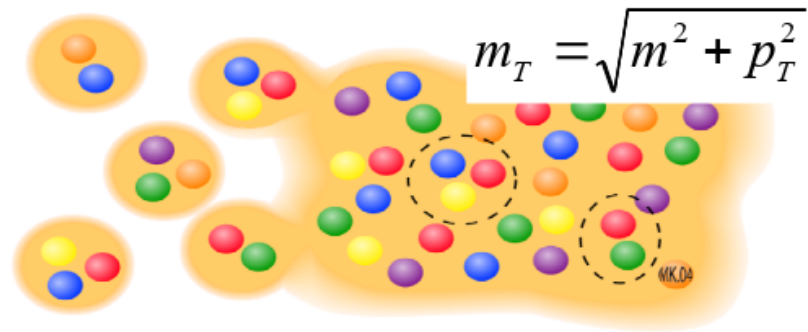
- -  $\pi^+\pi^-$ : min.bias, 0-10%,10-20%,20-30%,30-40%,40-50%,20-60%
- -  $K^+K^-$ : min.bias, 0-10%,10-20%,20-30%,30-40%,40-50%,20-60%
- + -  $p+p$ : min.bias, 0-10%,10-20%,20-30%,30-40%,40-50%,20-60%
- ▼ -  $d$ : min.bias, 10-50%
- △ -  $\phi$ : 20-60%

**STAR** (Phys. Rev. Lett. 92, Phys. Rev. C 72 (2005), Preliminary QM05, SQM06)

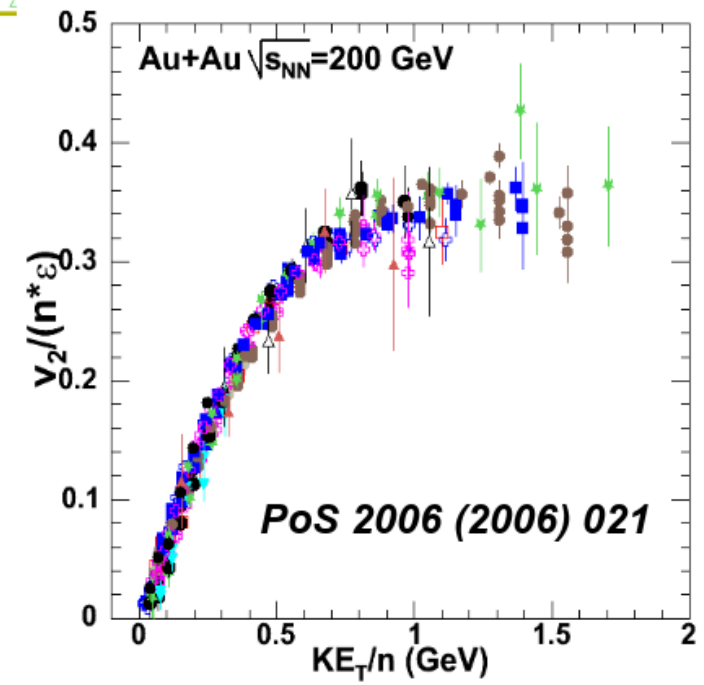
- -  $\pi^+\pi^-$ : min.bias
- ★ -  $K_S^0$ : min.bias, 5-30%,30-70%
- + -  $p+p$ : min.bias
- -  $\Lambda+\bar{\Lambda}$ : min.bias, 5-30%,30-70%
- -  $\Xi+\bar{\Xi}$ : min.bias
- ▲ -  $\Omega+\bar{\Omega}$ : min.bias

$$KE_T = m (\gamma_T - 1)$$

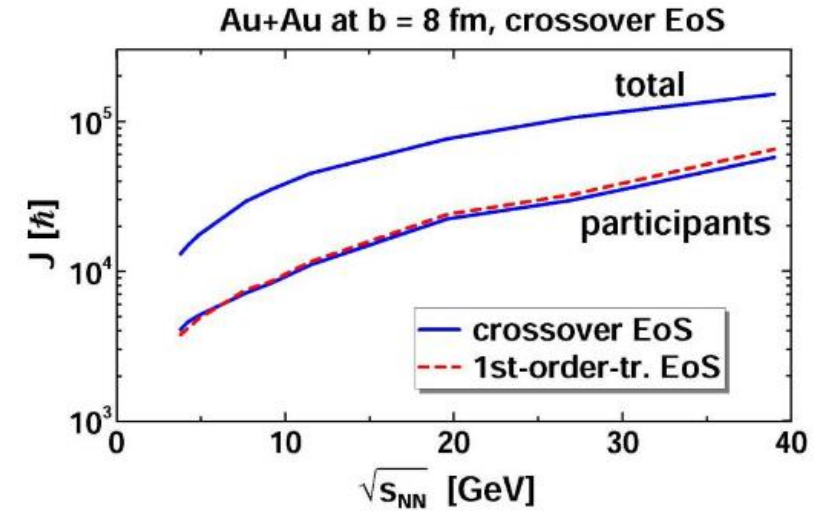
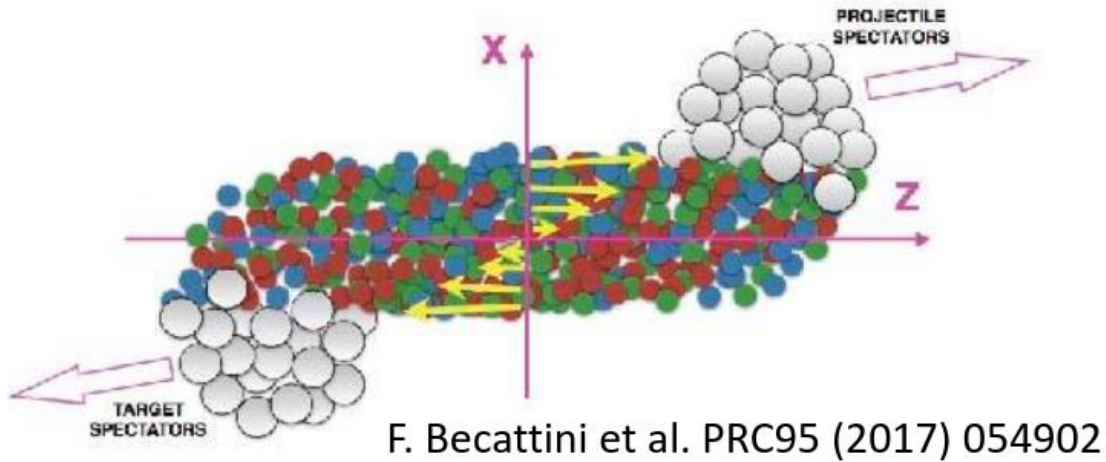
$$= m_T - m$$



**n=2 for mesons and n=3 for baryons**



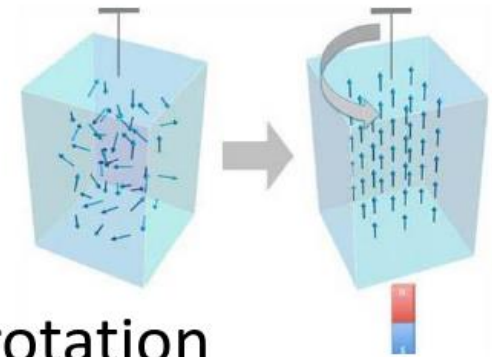
# Vortical motion of nuclear matter



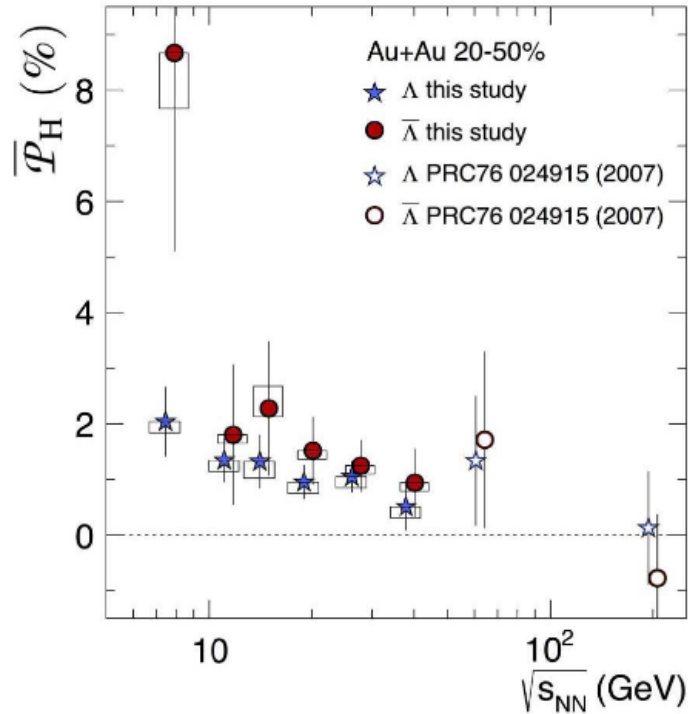
Vortical motion:  $\boldsymbol{\omega} = (1/2) \nabla \times \mathbf{v} = \mathbf{Vorticity}$

Relativistic Vorticity =  $\omega_{\mu\nu} = \frac{1}{2} (\partial_\nu u_\mu - \partial_\mu u_\nu)$

- Angular momentum  $\rightarrow$  spin polarization
- Similarly to Barnett effect (1915): magnetization by rotation



# Polarization Measurements



**STAR**

- ✓ Global  $\Lambda$  and anti- $\Lambda$  polarization [[Nature 548, 62 \(2017\)](#)]
- ✓ Local polarization of hyperons along the beam direction [[PRL 123, 132301 \(2019\)](#)]
- ✓ Measurement of global spin alignment of vector Mesons [[NPA 1005 \(2021\) 121733](#)]
- ✓ Global polarization of  $\Xi$  and  $\Omega$  hyperons at 200 GeV [[PRL 126 \(2021\) 16, 162301](#)]

**At NICA and FAIR energies, data are still very scarce**

- HADES:  $\Lambda$  Polarization at 2.4 GeV [[PLB 835 \(2022\) 137506](#)]
- STAR-FXT:  $\Lambda$  Polarization at 3 and 7.2 GeV [[PRC 104 \(2021\) L061901](#); [EPJ Web Conf. 259, 06003 \(2022\)](#)].

Global polarization is measured from the angular distributions of hyperon decay product:

$$P_H = \frac{8}{\pi\alpha_H} \frac{\langle \sin(\Psi_1 - \phi_d^*) \rangle}{\text{Res}(\Psi_1)}$$

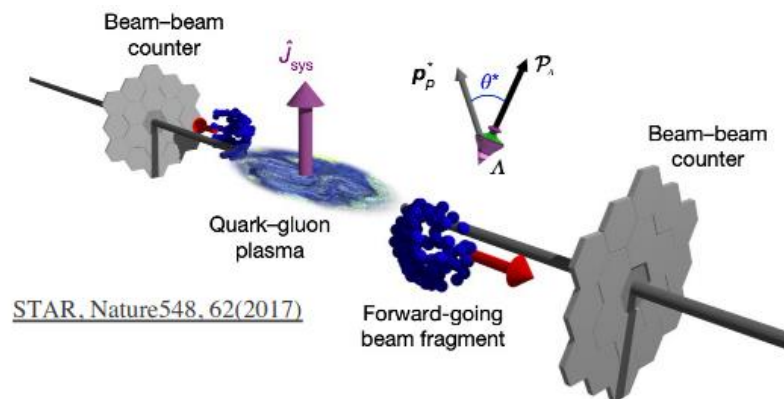
Thermal vorticity:

$$\omega = k_B T (P_\Lambda + P_{\bar{\Lambda}}) / \hbar \quad \omega \sim (9 \pm 1) \times 10^{21} \text{ s}^{-1}$$

# STAR ☆ Global Polarization in BES and FXT

STAR, arXiv:2108.00044

The average vorticity points along the direction of the angular momentum of the  $\hat{J}_{sys}$



Global polarization is measured from the angular distributions of hyperon decay product:

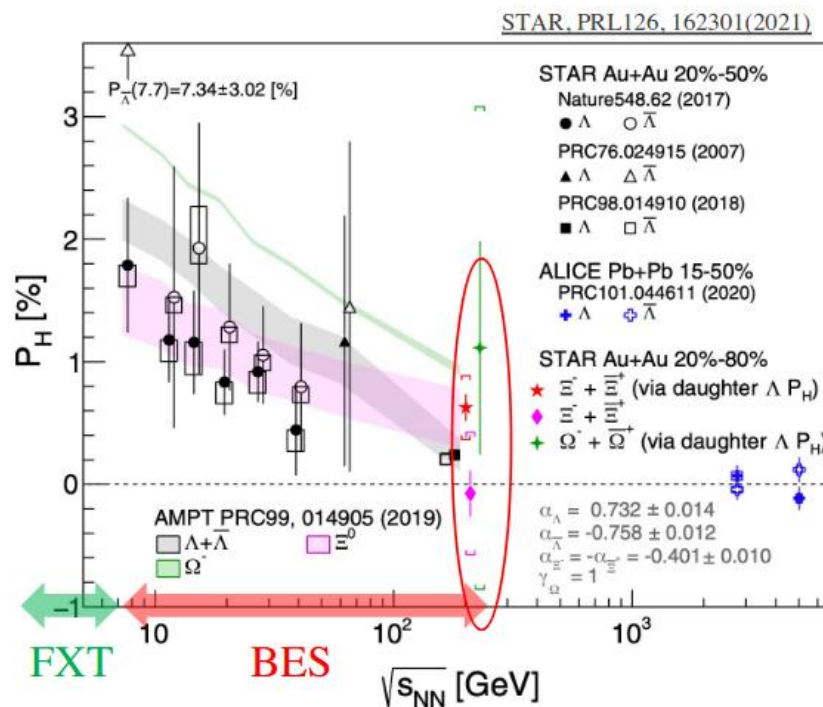
$$P_H = \frac{8}{\pi\alpha_H} \frac{\langle \sin(\Psi_1 - \phi_d^*) \rangle}{\text{Res}(\Psi_1)}$$

Thermal vorticity:

$$\omega = k_B T (P_\Lambda + P_{\bar{\Lambda}}) / \hbar \quad \omega \sim (9 \pm 1) \times 10^{21} \text{ s}^{-1}$$

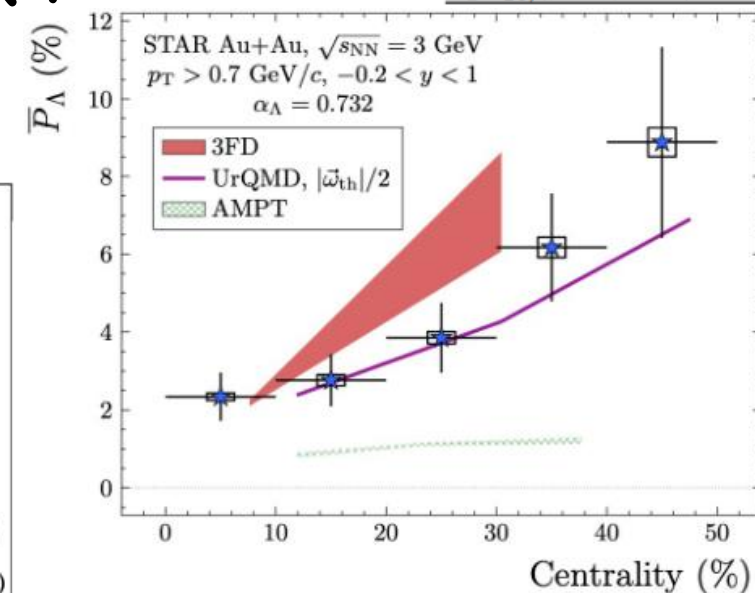
F. Becattini et al., PRC95, 054902(2017)

Opens up new directions in the study of the hottest, least viscous and most vortical fluid matter.



Large angular momentum transferred by the two colliding nuclei

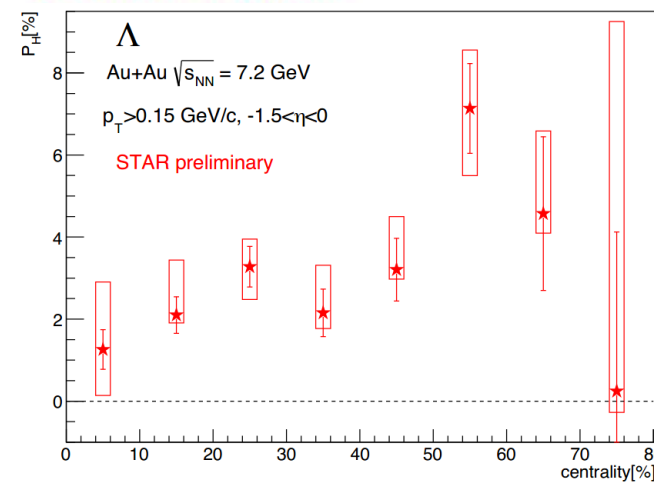
Stronger polarization at lower collision energies.



Much larger  $\bar{P}_\Lambda$  in FXT 3 GeV at 20-50%

$$4.91 \pm 0.81 \text{ (stat.)} \pm 0.15 \text{ (syst.)} \%$$

Larger hyperon polarization for more peripheral collisions



# Correlation Femtoscopy

- **Two-particle correlation function (CF):**

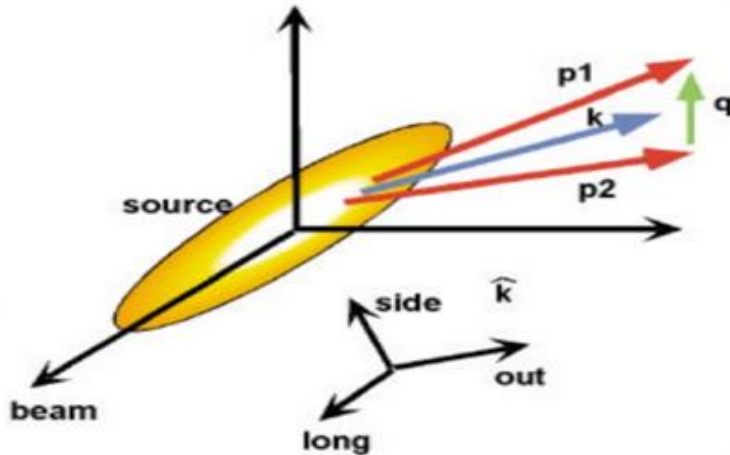
$$CF(p_1, p_2) = \int d^4r S(r, k) |\Psi_{1,2}(r, k)|^2$$

$r = x_1 - x_2$  and  $q \equiv q_{inv} = p_1 - p_2$

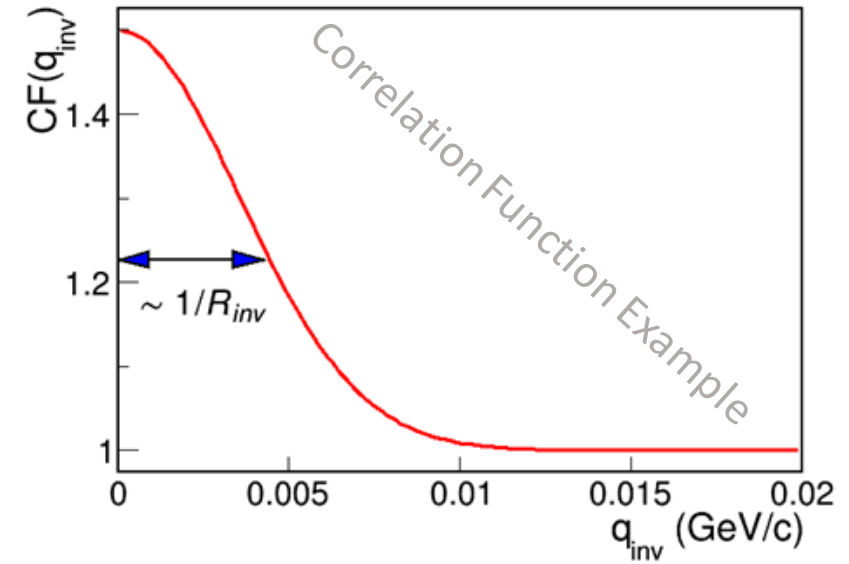
- **Experimentally:**

$$CF(q) = A(q)/B(q)$$

- $A(q)$  – contain quantum statistical (QS) correlations and final state interactions (FSI)
- $B(q)$  – obtained via mixing technique (does not contain QS and FSI)



S. Pratt. PRD 33 (1986) 1314  
G. Bertsch. PRC 37 (1988) 1896



The relative pair momentum can be projected onto the Bertsch-Pratt, **out-side-long system**:

$q_{long}$  – along the beam direction

$q_{out}$  – along the transverse momentum of the pair

$q_{side}$  – perpendicular to longitudinal and outward directions

Correlation functions are constructed in Longitudinally Co-Moving System (LCMS), where  $p_{1z} + p_{2z} = 0$

# Why Correlation Femtoscopy?

- Access to the spatial and temporal information about a particle-emitting source at kinetic freeze-out
- Different particle species are sensitive to various effects (Final State Interactions (FSI), transport properties, asymmetries, etc...)

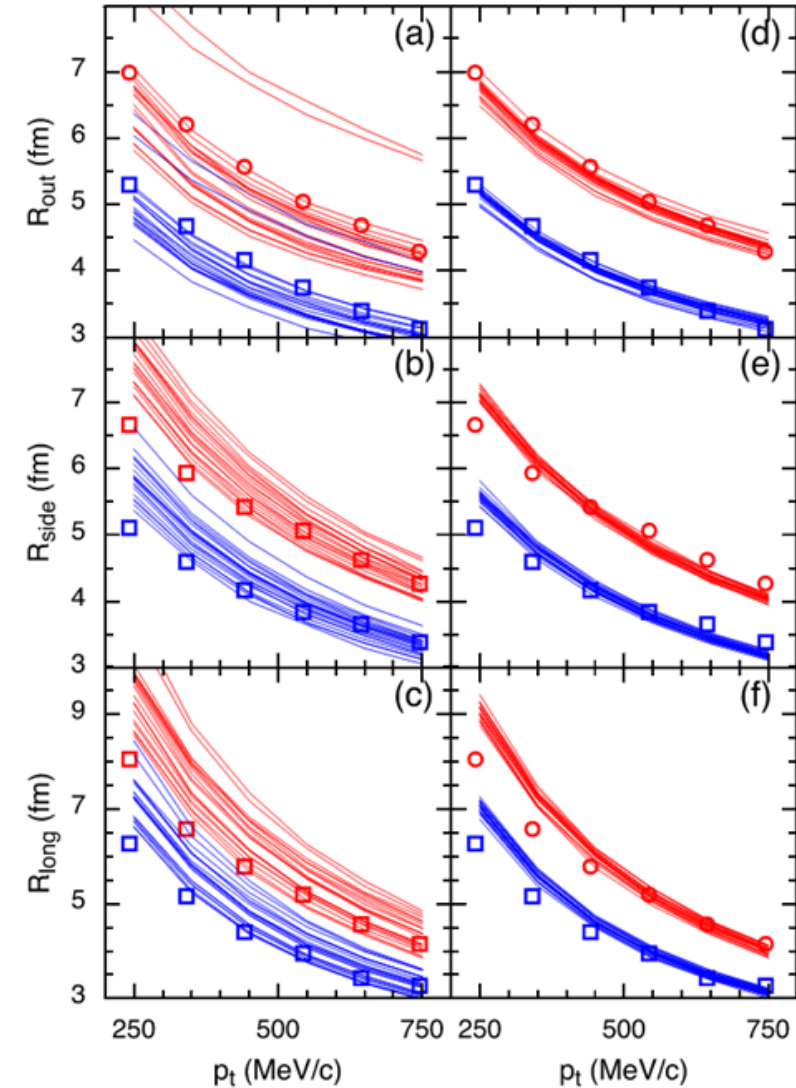
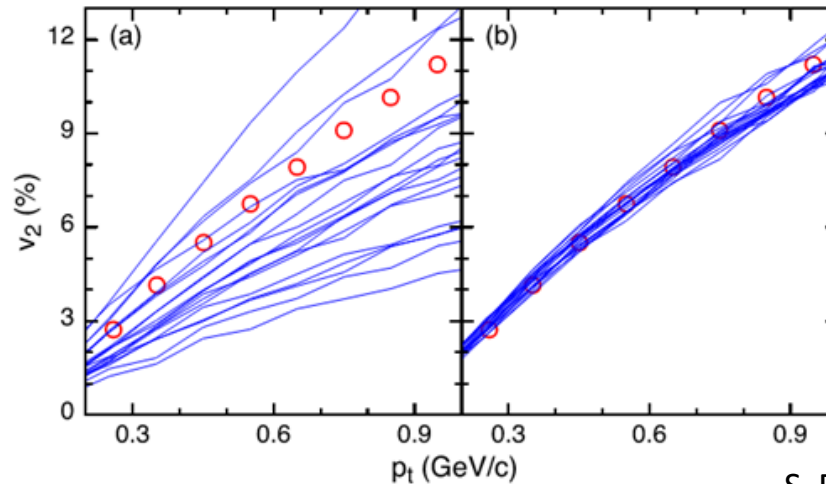
V.M. Shapoval et al. NPA 968 (2017) 391

M.A. Lisa et al. Ann. Rev. Nucl. Part. Sci. 55 (2005) 357

D.H. Rischke, M. Gyulassy. NPA 608 (1996) 479

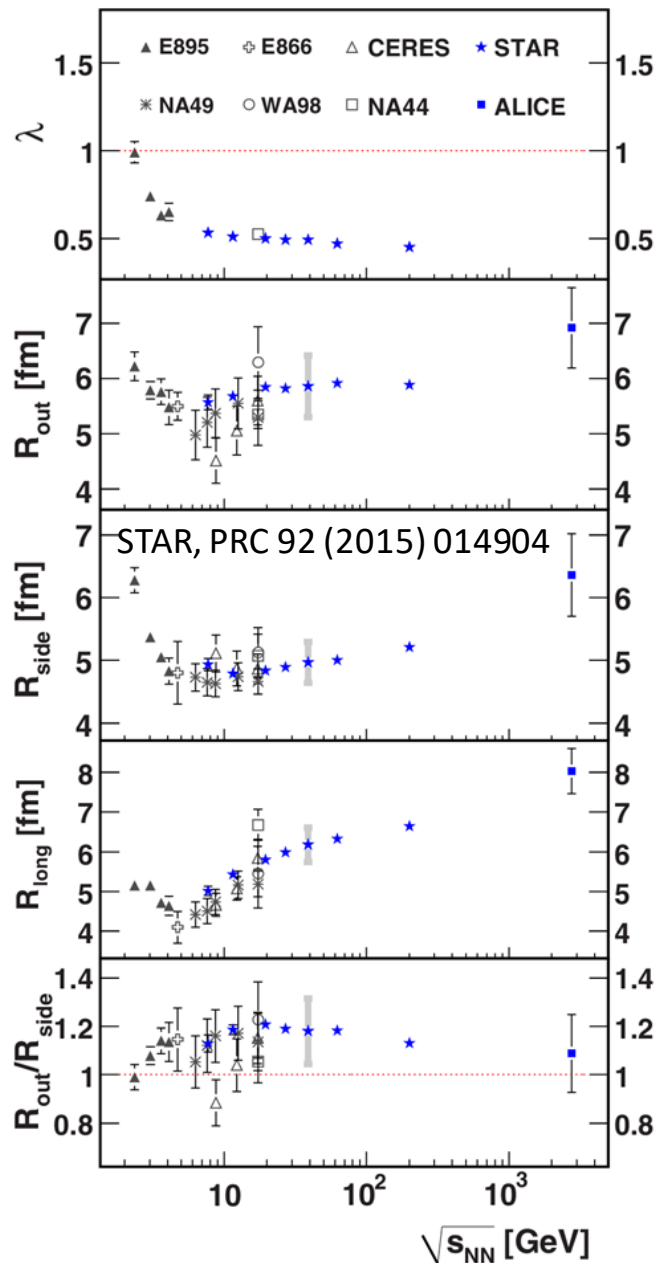
R. Lednicky et al. Phys. Lett. B 373 (1996) 30

- Strong model constraints

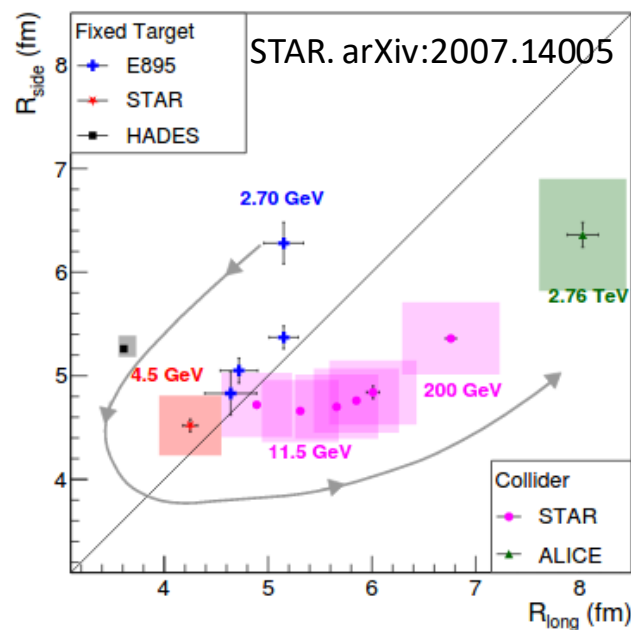


S. Pratt et al. PRL 114 (2015) 202301

# Femtoscscopy: World Systematics

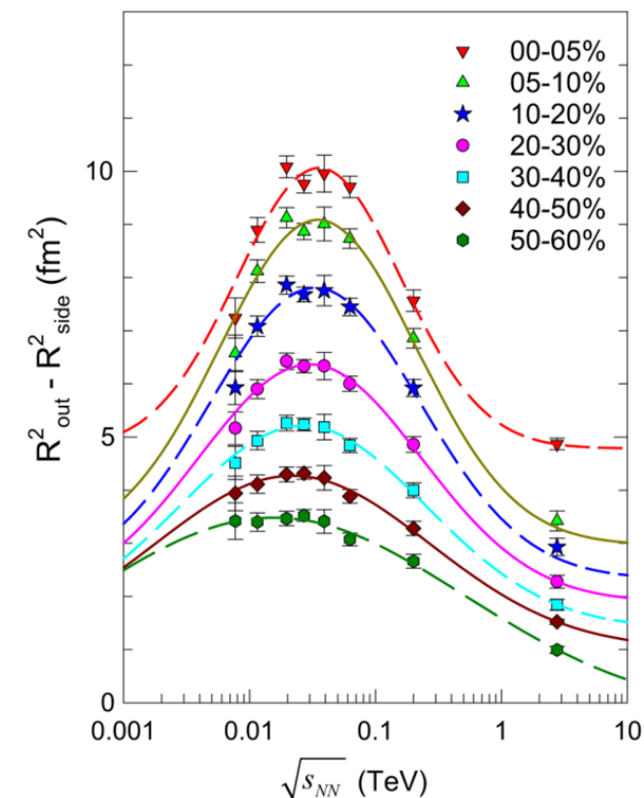


- Precise measurements in a broad energy range (from 7.7 GeV to 2.76 TeV)
- Need more high-statistics measurements at low energies
- Precise measurements exist only with pions
  - Need heavier particles



G. Nigmatkulov et al. ICPPA-2020

Lacey. PRL 114 (2015) 142301



# Summary

- Many exciting results from STAR
- Most of the physics measurements rely on the precise measurement of:
  - Collision centrality
  - Event plane
  - Particle momentum
  - Particle identification
- More results will appear soon for the data from the Beam Energy Scan II program



Thank you for your attention  
ध्यान देने के लिए आपका धन्यवाद